Summer sea-ice variability on the Antarctic margin during the last glacial period reconstructed from snow petrel (*Pagodroma nivea*) stomach-oil deposits

Erin L. McClymont[1], Michael J. Bentley[1], Dominic A. Hodgson[2,1], Charlotte L. Spencer-Jones[1], Thomas
Wardley[1], Martin D. West[1], Ian W. Croudace[3], Sonja Berg[4], Darren Gröcke[5], Gerhard Kuhn[6], Stewart
S.R. Jamieson[1], Louise Sime[2], Richard A. Phillips[2]

[1]Department of Geography, Durham University, Durham, DH1 3LE, United Kingdom.
[2]British Antarctic Survey, Natural Environment Research Council, Cambridge, CB3 0ET, United Kingdom.
[3]Ocean and Earth Science, University of Southampton, National Oceanography Centre, Southampton, SO14 3ZH, United
Kingdom.
[4]Institute of Geology and Mineralogy, University of Cologne, Cologne, D-50674, Germany.
[5]Department of Earth Science, Durham University, Durham, DH1 3LE, United Kingdom.
[6]Alfred-Wegener-Institut Helmholtz-Zentrum für Polar- und Meeresforschung, Bremerhaven, D-27568, Germany.

Correspondence to: Erin L. McClymont (erin.mcclymont@durham.ac.uk)

Abstract. Antarctic sea ice is a critical component of the climate system, affecting a range of physical and biogeochemical
feedbacks, and supporting unique ecosystems. During the last glacial stage, Antarctic sea ice was more extensive than today,
but uncertainties in geological (marine sediments), glaciological (ice core), and climate model reconstructions of past sea-ice
extent continue to limit our understanding of its role in the Earth system. Here, we present a novel archive of past sea-ice
environments from regurgitated stomach oils of snow petrels (*Pagodroma nivea*), preserved at nesting sites in Dronning Maud
Land, Antarctica. We show that by combining information from fatty acid distributions and their stable carbon isotope ratios
with measurements of bulk carbon and nitrogen stable isotopes and trace metal data, it is possible to reconstruct changing snow
petrel diet within Marine Isotope Stage 2 (ca. ~~22.6-28.8~~24.3-30.3 cal. kyr BP). We show that, as today, a mixed diet of krill
and fish characterises much of the record. However, between ~~25.7-26.8~~27.4-28.7 cal. kyr BP signals of krill almost disappear.
By linking dietary signals in the stomach-oil deposits to modern feeding habits and foraging ranges, we infer the use by snow
petrels of open water habitats ('polynyas') in the sea ice during our interval of study. The periods when consumption of krill
was reduced are interpreted to correspond to the opening of polynyas over the continental shelf, which became the preferred
foraging habitat. Our results challenge hypotheses that the development of extensive, thick, multi-year sea-ice close to the
continent was a key driver of positive sea ice-climate feedbacks during glacial stages, and highlight the potential of stomach-
oil deposits as a palaeo-environmental archive of Southern Ocean conditions.

1 Introduction

Antarctic sea ice is globally important: large seasonal fluctuations in its spatial extent influence planetary albedo, ocean-atmosphere exchanges of heat and climatically-active gases including CO_2, and the formation of intermediate and deep water masses which create the world's largest sink of heat and carbon (e.g. Ackley et al., 2015; Delille et al., 2014; Arrigo et al., 2008; Frölicher et al., 2011). Antarctic sea-ice extent is projected to decline by 16-67% by 2100 depending on greenhouse gas emission scenarios, but with low confidence due to a wide range of model responses (Collins et al., 2013).

The geological record offers an opportunity to set the relatively short (~50 yr) instrumental observations of sea ice into a longer-term context. During the Last Glacial Maximum (LGM, ~19-23 ka) (Tierney et al., 2020), the development of thick, multi-year and more extensive sea-ice is inferred from the disappearance of, or diagnostic changes in, assemblages of marine microfossils from many Southern Ocean sediment cores (e.g. Hillenbrand and Cortese, 2006; Grobe and Mackensen, 1993; Bonn et al., 1998; Lucchi et al., 2002; Gersonde et al., 2005; Benz et al., 2016; Collins et al., 2012; Allen et al., 2011). An expanded 'sea-ice cap' is proposed to have increased deep-ocean storage of CO_2, by limiting the air-sea gas exchange and by enhancing CO_2 export through increased Antarctic Bottom Water production (e.g. Stephens and Keeling, 2000; Ferrari et al., 2014).

Antarctic sea-ice environments today are dynamic and complex at a range of temporal and spatial scales (Parkinson, 2019; Turner et al., 2020), and include open waters within the sea-ice pack ('polynyas') which span a large size range (1000-~400,000 km^2 (Arrigo and van Dijken, 2003), are poorly represented in models (Mohrmann et al., 2021), and yet impact ocean circulation, sea ice formation and air-sea gas exchange (Mohrmann et al., 2021; Morales Maqueda et al., 2004). A similarly complex picture has emerged for the Last Glacial period: in the Atlantic sector of the Southern Ocean, spanning the Weddell, Lazarev and Scotia Seas (Fig. 1) there is fragmentary empirical evidence for polynyas during and before the LGM, as detailed by intervals of high productivity or bottom-current activity in marine sediment cores, and occupation of nesting sites by seabirds that require open water within their foraging range (e.g. Smith et al., 2010; Sprenk et al., 2014; Mackensen et al., 1989; Thatje et al., 2008; Berg et al., 2019; Weber et al., 1994). Millennial-scale variability in the extent of the seasonal sea-ice zone has also been described (Collins et al., 2012; Gersonde et al., 2003; Rae et al., 2018), but large (10-20%) uncertainties remain in both models and geological datasets (Collins et al., 2012; Roche et al., 2012; Gersonde et al., 2003). Maximum summer sea-ice extent was likely reached at 30-22 ka (Collins et al., 2012; Gersonde et al., 2003; Allen et al., 2011; Xiao et al., 2016), raising the possibility that Southern Ocean sea-ice / climate feedbacks were more important before the global LGM (Allen et al., 2011; Xiao et al., 2016).
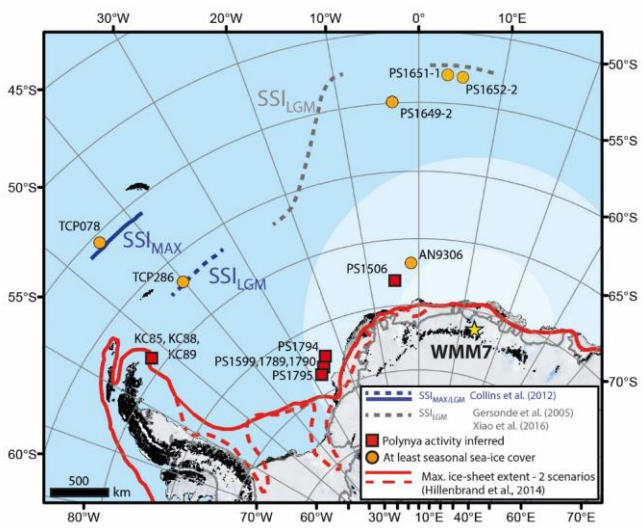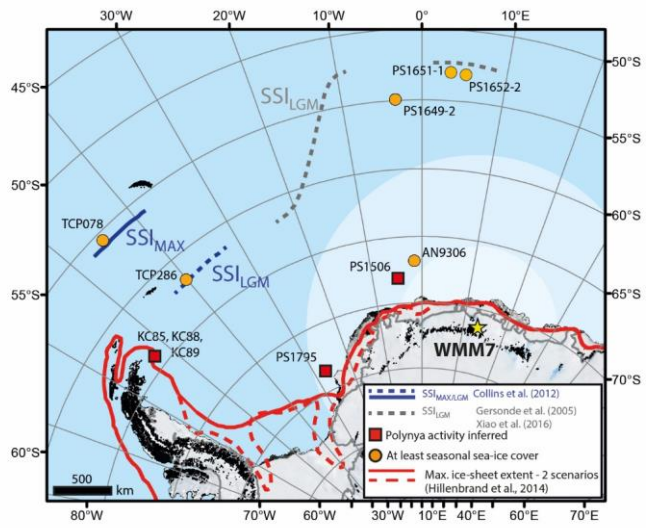
Figure 1: Sea ice records of the last glacial stage for the Atlantic sector of the Southern Ocean. The stomach-oil deposit presented here (WMM7) is shown by the yellow star (Untersee Oasis, 71° 22' S, 13° 19' E). The likely snow petrel foraging range is indicated by the shaded ellipse: although snow petrels can forage 2600 +/- 1000 km from their nests (pale shading) they are found in their highest densities within 700 km of the nest site during the breeding season (darker shading) (Delord et al., 2016). Boundaries of the maximum summer sea-ice extent (22-30 ka, Allen et al., 2011; Collins et al., 2012) and LGM summer sea ice extent (19-23 ka, Gersonde et al., 2005; Xiao et al., 2016) are marked. Sites where polynya activity has been inferred for the last glacial stage are shown in red (Bonn et al., 1998; Smith et al., 2010; Sprenk et al., 2014; Weber et al., 1994), noting that the KC sites (Smith et al., 2010) and south-east Weddell Sea sites (PS1599, 1789, 1790 and 1974 (Weber et al., 1994) and PS1795 (Sprenk et al., 2014)) infer polynyas opening 'upstream' of the core locations. Note that the continental shelf edge is effectively also delineated by the solid red line of LGM maximum ice-sheet extent.

Here, we investigate changes in the sea-ice environment during the time of proposed maximum sea-ice extent (30-22 ka) by analysing a sequence of preserved stomach oils of snow petrels (*Pagodroma nivea*). Although sometimes referred to as 'Antarctic mumiyo' (e.g. Berg et al., 2019; Thor and Low, 2011), this is a misnomer because its biological origin is so different from the original use of 'mumiyo' which was used to describe an organic, tar-like substance of unknown origin, found in high altitude rocks and caves especially in Asia (Hiller et al., 1988 and references therein; Aiello et al., 2011). We therefore refer to Antarctic 'stomach-oil deposits' here.

Progressive accumulation of regurgitated stomach oils at the entrance to snow petrel nests in rock crevices and scree slopes (e.g. Johansson and Thor, 2004) leads to stratified deposits which may span several millennia (Hiller et al., 1988; Wand and Hermichen, 2005; Hiller et al., 1995; Thor and Low, 2011; Berg et al., 2019). The deposits include a mixture of stomach oils, guano, aeolian dusts and other mineral matter (Berg et al., 2019). Snow petrels forage in open waters at the margins of, or amongst, the sea ice, within a restricted range (several 100 km) from their nesting sites (Delord et al., 2016; Marchant and Higgins, 1990). Snow petrels feed on fish, krill and squid (Ainley et al., 1984; Delord et al., 2016), and the stomach oils preserve a biochemical fingerprint of these prey. For example, krill tend to have high abundances of $C_{14:0}$, $C_{16:0}$ and $C_{18:1}$ fatty acids and a variety of carotenoid pigments (e.g. Cripps et al., 1999; Färber Lorda and Ceccaldi, 2020), as well as Cu, Zn and Fe (Rainbow, 1989; Palmer Locarnini and Presley, 1995; Liu et al., 2013), whereas squid and fish are dominated by $C_{16:0}$ and $C_{18:0}$ fatty acids, respectively (Lewis, 1966). The presence of Cu in crustaceans (including krill) is linked to hemocyanins in invertebrate blood (Bridges et al., 1983), which provide an alternative oxygen carrier to the hemoglobins of vertebrate blood. Stable isotope ratios provide useful proxies for trophic level (δ^{15}N) and foraging habitat (δ^{13}C), enabling diet comparisons between snow petrels and other seabirds (Delord et al., 2016; Cherel et al., 2010; Steele, 2005; Phillips et al., 2011).

Here, we undertake elemental scans, organic geochemistry and stable isotope analysis to investigate snow petrel diet during the Last Glacial stage from a stomach-oil deposit collected at Lake Untersee in central Dronning Maud Land (DML). Since snow petrels have a restricted foraging range during the breeding season (Delord et al., 2016), our analyses enable us to reconstruct changes in their diet and foraging habitat relatively close to the Antarctic margin (Fig. 1). In turn, we hypothesise

100 that the biochemistry of the stomach-oil deposits provides diagnostic signatures of snow petrels foraging in sea -ice over or beyond the continental shelf, and in polynyas, offering novel insights into the evolution of sea-ice environments during the last glacial stage.

2 Materials and Methods

2.1 Untersee Oasis sequence WMM7 and its regional context

105 The stomach-oil deposit WMM7 was collected during the GeoMaud expedition (1995/1996), from the Untersee Oasis (71° 21.6' S, 13° 18.96' E) in DML (Fig. 1) (Wand and Hermichen, 2005). The deposit was retrieved from under a boulder on a steep slope west of Lake Untersee, c. 320 m above the lake surface, at an elevation of 880 m above sea level. WMM7 was kept in dark, cold storage (4°C, 60% humidity) at the Alfred Wegener Institute, Germany, until analysis. The sample had a waxy consistency, so to preserve its internal structure it was frozen immediately before slicing and sub-sampling at Durham
110 University. A central slab of WMM7 was sectioned for non-destructive, high-resolution X-ray fluorescence (XRF) analysis (40 mm thick, 50 mm wide and 150 mm long, marked on Fig. 2a). Samples for stable isotope and lipid analysis were taken from adjacent to the XRF slab (Fig. 2a).

Before sub-sampling, WMM7 weighed c. 1 kg, and was 155-194 mm thick, 144 mm wide, and 120 mm deep (Fig. 2a). It had
115 an irregular, mammillated outer surface, but was characterised internally by mm-scale laminae that were traced through the deposit. The laminae visibly slope away from the centre of the deposit, showing that the deposit progressively draped over the underlying rock. Three distinct units were observed in the sequence during sampling (Fig. 2b): the oldest part of the sequence, (160-110 mm depth, Unit III) was characterised by laminated, yellow-brown deposits, overlain by a zone of relatively dark, brown-black deposits with more poorly defined laminae (Unit II). The Unit II/I transition was gradual (80-70 mm), and Unit I
120 contained yellow-brown deposits with sub-mm scale laminae (Unit I). No hiatuses were visible in the stratigraphy, which would be indicated by breaks in the structure or visible sediment which would have beed deposited and concentrated during an interval when stomach oils were not being deposited. The linear age model (Fig. 2) also indicated continuous accumulation.
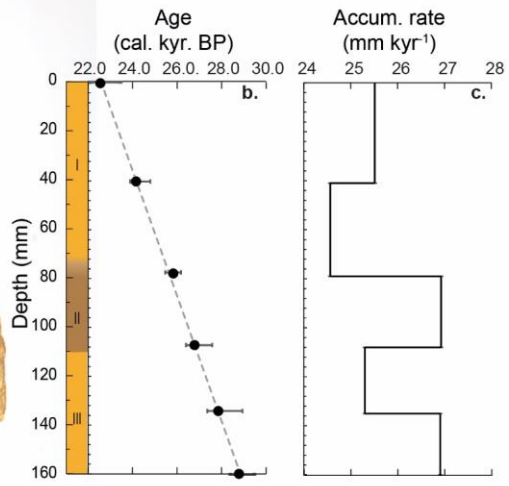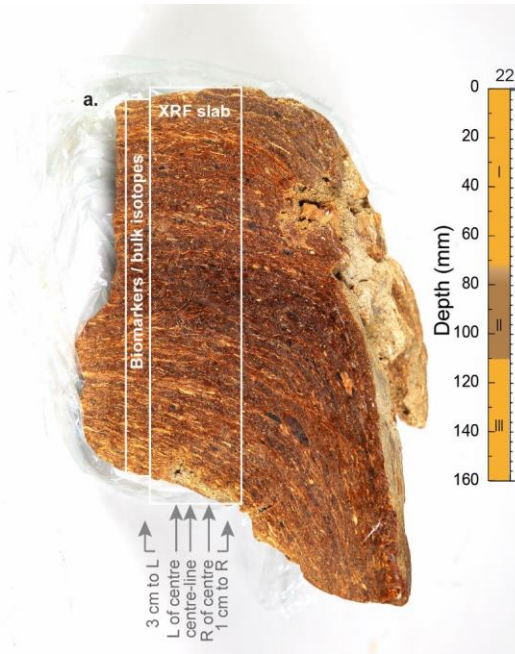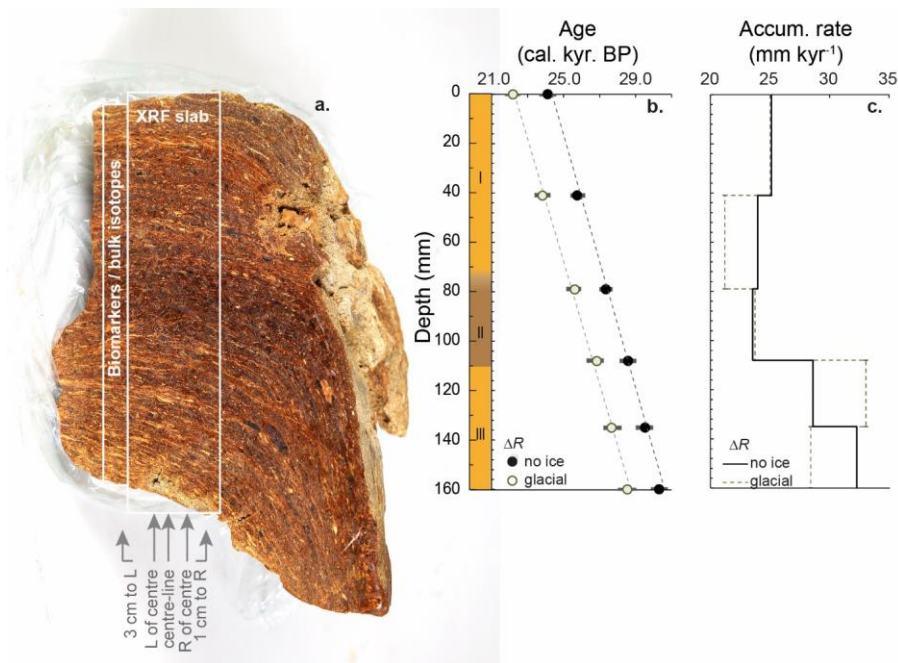
Figure 2: Stomach-oil deposit WMM7 stratigraphy and age-depth model. (a.) cross-section of the section used for sub-sampling, scaled with panels (b) and (c). Note the clear laminae which slope to the right away from the main slab. A zone of darker brown and less well defined laminae is found in the central section (Unit "II" in panel (b)). A 5 cm wide slab was cut for XRF analysis. Data from the centre-line scan is shown in Fig. 3 and used for statistical analysis. The results of additional scans to the left and right of centre, and from two new cuts (3cm left, 3 cm right; see arrows) and shown in Figure ~~B1~~A1. Biomarker and bulk stable isotope samples were taken immediately to the left of the XRF slab. (b.) and calibrated using either a Holocene "no sea ice" ΔR or a glacial-stage "maximum sea ice" ΔR (see Table 1 for ¹⁴C calibration). Figs. 3-6 apply the Holocene "no ice" ΔR age model; (c.) accumulation rate between age control points for the two age-model scenarios. ~~three-unit stratigraphy and age-depth model constrained by 6 bulk radiocarbon dates (see Table 1 for ¹⁴C calibration). (c.) accumulation rate between age control points.~~ Linear interpolation was applied to generate an age-depth model for all sampling points.

2.2 Radiocarbon analysis

Previous ^{14}C analysis of the top of WMM7 provided a age constraint of 21,551 ± 110 yr (Berg et al., 2019). To establish an age-depth model, six additional bulk samples were dated (Table 1), and linear interpolation was applied between dating points. Each sample was digested in 2M HCl (80°C, 8 hours), washed free from mineral acid with deionised water, then dried. Samples were graphitized using an automated graphitization system (Rethermeyer et al., 2019) and analysed for ^{14}C by accelerator mass spectrometry (AMS) at CologneAMS, Germany. Radiocarbon ages were converted to calendar ages (Table 1) using the MARINE20 radiocarbon age calibration (Heaton et al., 2020), adopting two approaches to explore the potential influence of

changing sea-ice extent on ΔR (Heaton et al., 2021). First, radiocarbon ages were corrected for the Southern Ocean marine reservoir effect by applying a ΔR of 670 yr ± 50 yr from pre-bomb ^{14}C ages at Hope Bay in the western Weddell Sea (Björck et al., 1991). As this ΔR reflects Holocene conditions, where sea ice is low or absent from the region, this calibration is described as a "no sea ice" scenario (Table 1; Heaton et al., 2021). As variable sea-ice extent introduces additional uncertainty to radiocarbon age calibration in polar regions (Heaton et al., 2020), a second scenario was explored, applying a modelled glacial-stage maximum sea ice ΔR of 2480 ± 50 yr (Table 1). As snow petrels forage in surface waters within sea ice or close to the sea-ice edge, we suggest the glacial stage ΔR is likely an over-estimate. For the results presented here, the datasets are described according to the Holocene "no sea ice" age model (Table 1), recognising that this provides a maximum age for the WMM7 record. This approach also ensures that our results can be incorporated into studies using stomach-oil deposits for constraining ice-sheet thinning histories, where they are used to indicate the onset of ice-free conditions (e.g. Hiller et al., 1998; Hillenbrand et al., 2014 and references therein). Radiocarbon ages were converted to calendar ages (Table 1) using the MARINE13 radiocarbon age calibration (Reimer et al., 2013) corrected for the Southern Ocean marine reservoir effect by applying a ΔR of 880 yr ± 100 yr from pre-bomb ^{14}C ages at Hope Bay in the western Weddell Sea (Björck et al., 1991; Sterken et al., 2012). We apply MARINE13 here since MARINE20 is not recommended for polar regions with variable sea-ice extent (Heaton et al., 2020). A comparison of the two approaches for WMM7 yields calibrated ages which are within error (Table A11) and thus do not affect our interpretations or conclusions. However, we acknowledge that the application of a constant, modern ΔR to a region affected by greater sea-ice extent during MIS 2 leads to larger uncertainty and potential bias in our calendar ages than indicated by the results in Table 1 (Heaton et al., 2020; Heaton et al., 2021).

Table 1 Radiocarbon dates and calibrated ages. All ^{14}C analyses were performed on bulk samples at CologneAMS, Germany. COL3022 was previously published (Berg et al., 2019). Calibration to calendar ages used MARINE13 (Reimer et al., 2013), and ΔR of 880 ± 100 yr (Björck et al. 1991), following Sterken et al. (2012).

Depth (mm)	Unit	AMS Lab ID	Median Age (^{14}C yr BP)	+/- (^{14}C yr BP)	Calibrated age (cal. yr BP) MARINE13, ΔR 880 ±100 yr	+/- (cal. yr BP, 2σ)
0	I	COL3022	21,550	110	22,400	894 / 383
0	I	COL4327	21,660	104	22,550	905 / 399
40	I	COL4326	23,170	114	24,160	637 / 272
79	I/II	COL4328	24,790	115	25,710	466 / 240
108	II/III	COL4329	25,980	133	26,780	786 / 385
135	III	COL4325	26,920	149	27,850	1085 / 497
160	III	COL4324	27,730	148	28,780	686 / 386

Table 1 Radiocarbon dates and calibrated ages. All ^{14}C analyses were performed on bulk samples at CologneAMS, Germany. COL3022 was previously published (Berg et al., 2019). All calibrations to calendar ages used MARINE20 (Heaton et al., 2020). To explore the likely range of impacts of sea ice on our ^{14}C calibrations, we first apply the nearest Holocene ΔR of 670 ± 50 yr (Björck

et al. 1991) which assumes low/absent sea ice sampled by WMM7 ($\Delta R^{Holocene}$). A second calibration ($\Delta R^{glacial\ stage}$) assumes enhanced sea-ice cover, as suggested for the last glacial stage, generated by adding 1800 yr of additional ocean ^{14}C depletion as suggested by Heaton et al. (2020, 2021).

Depth (mm)	Unit	AMS Lab ID	Median Age (^{14}C yr BP)	+/- (^{14}C yr BP)	Calibrated age (cal. yr BP) MARINE20, $\Delta R^{Holocene}$ 670 ±50 yr	Calibrated range (2σ)	Calibrated age (cal. yr BP) MARINE20, $\Delta R^{glacial\ stage}$ 2470 ±50 yr	Calibrated range (2σ)
0	I	COL3022	21,550	110	23987	23668-24366	22061	21736-22358
0	I	COL4327	21,660	104	24124	23758-24495	22171	21859-22492
40	I	COL4326	23,170	114	25760	25488-26091	23810	23502-24167
79	I/II	COL4328	24,790	115	27350	27093-27614	25603	25263-25868
108	II/III	COL4329	25,980	133	28585	28215-28938	26825	26389-27126
135	III	COL4325	26,920	149	29531	29116-29867	27642	27266-28057
160	III	COL4324	27,730	148	30307	29949-30685	28522	28105-28912

2.3 XRF analysis

XRF analysis was performed using the ITRAX core scanner at the National Oceanography Centre, Southampton, U.K. (Croudace et al., 2006). A molybdenum X-ray source was used (45 kV, 40 mA), at a step size of 200 µm and exposure time of 400 secs per increment. To test for potential contamination during sub-sampling, and to explore internal consistency of the recovered signals, a further 5 profiles were measured on the central slab (Fig. 2a, Figure BA1). Multiple XRF scans confirmed that the major patterns outlined below are consistently recorded in WMM7, with differences accounted for by changes in the orientation and spatial continuity of the laminae (Figure AB1).

2.4 Bulk organic matter elemental composition and stable isotope analysis

Directly adjacent to the left margin of the XRF slab, 15 contiguous 10 mm sub-samples were taken by scalpel for bulk stable isotope analysis (Fig. 2a). Carbon and nitrogen stable isotope analyses were performed using a Costech Elemental Analyser

(ECS 4010) connected to a Thermo Scientific Delta V Advantage isotope ratio mass spectrometer. Carbon isotope ratios are corrected for ^{17}O and reported in standard delta (δ) notation in per mil (‰) relative to Vienna Pee Dee Belemnite (VPDB). Nitrogen isotope ratios are reported against atmospheric nitrogen (AIR). Isotopic accuracy was monitored through multiple daily analysis of international (e.g., IAEA-600, IAEA-CH-3, IAEA-CH-6, IAEA-N-1, IAEA-N-2, NBS 19, USGS24, USGS40) and in-house standards, which provided a linear range for δ^{13}C between –46 ‰ and +3 ‰ and for δ^{15}N between –4.5 ‰ and +20.4 ‰. Analytical uncertainty was typically ±0.1 ‰ (2 sd) for replicate analyses of the international standards and <0.2 ‰ (2 sd) on replicate sample analysis. Total organic carbon (TOC) and nitrogen data was obtained as part of the isotopic analysis using the internal standard, glutamic acid (40.82 wt% C, 9.52 wt% N).

2.5 Biomarker distributions and stable carbon isotope analysis

A 2 mm stainless steel dermal punch was used to extract samples for biomarker analysis, from the same line as the bulk stable isotope samples (Fig. 2a), including triplicates at 1 cm depth and 8 cm depth. Lipids were extracted from 0.03-0.3 g of each sample using repeated ultra-sonication (3 x 10 mins) in 10 ml dichloromethane/methanol (3:1), following addition of two internal standards of known concentration (androstanol, hexatriacontane). Ultrasonic extraction yielded between 16-43 mg total lipid extract.

An aliquot of the total lipid extract was dissolved in acetone, and analysed by UV-Vis spectrophotometry using a Dionex HPLC Quaternary pump and photo-diode array detector (McClymont et al., 2007). A grass standard and blank acetone were injected regularly to monitor potential instrument drift. The relative absorbance at wavelengths characteristic of chlorophyll derivatives ('chlorins') and potential carotenoid derivatives, at 410, 435 and 665 nm (Jeffrey et al., 1997) was calculated for each sample:

$$P\lambda = \frac{(A\lambda \; x \; DF)}{M}$$
(1)

Where Pλ = relative magnitude of absorbance for a given wavelength (abs. g-1); Aλ = integrated area for that wavelength, averaged over three repeat measurements; DF = dilution factor i.e. the aliquot of the total sample injected; M = mass of material which was extracted. To take into account the potential influence of variable organic matter deposition or preservation, we also normalised all photosynthetic pigment absorbance to TOC content (generated from section 2.4). There may be multiple sources of our target pigments (Jeffrey et al., 1997), so we refer to them as P410, P435 and P665 respectively, to identify the trends in absorbance for each specific wavelength.

The remaining extracts were saponified using 2 ml KOH (8%) in methanol (95%) and heated for 2 hours at 70°C. Neutral lipids were extracted using hexane; the remaining extracts were acidified using 2 M HCl, and the fatty acids were extracted using hexane. An internal standard of known concentration (heptadecanoic acid, 0.4 mg ml-1) was added to the fatty acid fractions, before generating fatty acid methyl esters (FAMEs) by methylating with 3 ml methanol: HCl (95: 5) for 12 hours at

70°C, then allowing to cool to room to temperature. After adding 4 ml of DCM-rinsed H2O to each sample, FAMEs were
215 recovered sequentially using hexane followed by hexane: dichloromethane (4:1) and pooled. FAME fractions were then taken
to dryness in a stream of N_2. The isotopic value of the methanol was determined through methylation of a phthalic acid with
known isotopic value (Lee et al., 2017).

The FAMEs were identified and quantified with a Thermo Trace 1310 gas chromatograph linked to an ISQ LT single
220 quadrupole mass spectrometer (GC-MS). Chromatographic separation was performed with a Restek Famewax
30m×0.25mm×0.25µm column. Sample extracts were injected (0.8µL) in CT split mode (80:1 ratio) into a PTV injector at
230°C with a constant helium carrier gas flowrate of 1.5ml/min. The oven temperature was initially set to 100°C for 3.0 min,
then ramped at 2°C/min to 230°C, and held at 230°C for 10 min. The transfer line temperature was set to 230°C and the ion
volume temperature to 220°C. A mass range of 38 to 600 m/z was scanned every 0.5 seconds giving at least 20 data points per
225 compound peak. Samples were identified and quantified by comparison to a Supelco 37 component ME mix (CRM47885,
Sigma-Aldrich) with peak area ratios calculated with reference to the peak area of the internal standard. Spectral confirmation
was performed using a NIST EI reference library.

The carbon isotopic compositions ($\delta^{13}C$) of individual saturated FAMEs were determined on 8 samples (22-132 mm depth)
230 using a Thermo GC-C-IRMS system at the Department of Geography, Durham University. All samples were run in duplicate.
The system was composed of a Trace 1310 GC coupled to a Thermo Delta V Plus via a GC IsoLink II and a Restek Famewax
30m×0.25mm×0.25µm column. Samples were injected (2µL) in splitless mode into a S/SL injector set to 240°C with a helium
carrier gas flowrate of 1.5ml/min. The oven temperature was initially set to 50°C for 1 min, then ramped to 100°C at 10°C/min,
then ramped to 240° at 3°C/min, and finally held for 10 min at 240°C. The alumina (with CuO,NiO and Pt wires) combustion
235 reactor was operated at 1000°C and conditioned with oxygen each day immediately before use. CO_2 reference gas pulses were

introduced at the start and end of each chromatogram to provide an isotope ratio reference point and to check the system
stability during the run. All the quantified FAME peaks in the selected carbon range were baseline resolved apart from the *cis*
and *trans* isomers of $C_{18:1}$. A FAME standard (CRM47885 - Supelco 37 component mix, Sigma-aldrich) was run with each
batch of isotope reference standards to confirm the retention time of the FAME peaks. Individual FAME isotope ratio values
240 were corrected using a multipoint linear normalization of a C_{14}-C_{20} FAME reference material (F8-3 standard provided by A.
Schimmelmann, Indiana University, Bloomington). Reference standard FAMEs from C_{14}-C_{20} were used to generate the
normalization curve, covering $\delta^{13}C$ values from −23.24 to −30.92 ‰. Reference material F8-3 was also used to determine the
usable amplifier signal range, which minimized the residuals, and gave an *r2* value of at least 0.995 for the normalization plot.
The concentration of the F8-3 FAME standard used for the linear normalization was adjusted to obtain reference amplifier
245 intensities within this range (1000 to 6000 mV). Each sample was then diluted and pre-run to determine the optimum solvent
volume required to fit within the amplifier signal range of the reference standards. The long term pooled standard deviations
of the ME F8-3 reference compounds were all <0.35‰ (ranging from 0.21 to 0.34‰, n=21). Fatty acid $\delta^{13}C$ was calculated

through mass balance corrections of the measured FAME $\delta^{13}C$ and known $\delta^{13}C$ of the added methyl group (Lee et al., 2017) and reported relative to Vienna PeeDee Belemnite (V-PDB).

2.6 Statistical analysis

Principal component analysis (PCA) was performed to investigate the potential for co-evolving relationships in the stomach oil geochemistry, using the PAST3 software (Hammer et al., 2001). We focussed on the XRF data for PCA since it was analysed at the highest resolution and with the highest number of variables, and used the variance-covariance matrix since all variables were measured in the same units (i.e. counts). Elements which consistently recorded counts below 500 were excluded from the analysis.

Cluster analysis was performed to identify units of similar geochemical composition using the *rioja* package in *R 3.6.0* (Juggins, 2020), whereby a hierarchical clustering is performed, constrained by sample order, and to a broken-stick model of a random distribution of zones within a sequence (Bennett, 1996). Due to the different sampling resolutions of the geochemical methods employed here, we re-sampled the XRF data by averaging element counts across the same depth-window sampled by each of the discrete geochemical measurements (10 mm diameter). This re-sampling approach does not alter the main signals of the principal components, although additional clusters are identified using the original XRF data (Figure BC1). We present the re-sampled XRF PCA here as an independent measure of geochemical change that is comparable to the resolution of the lipid distribution and stable isotope signatures.

3 Results

3.1 WMM7 age model

Stomach-oil deposit WMM7 spans 23,987 (23,668-24,366) 22,550 +905/-399 cal. yr B.P. through 30,307 (29,949-30,685) 28,780 +686/-386 cal. yr B.P. using the Holocene "no sea ice" ΔR for calibration (Table 1). The unit transitions are well constrained by ^{14}C-dates (Fig. 2b). The accumulation rate is remarkably stable, at at 26.6±3.7 mm cal. kyr^{-1} 25.8±1.0 mm cal. kyr^{-1} (Fig. 2c).

3.2 Elemental composition (XRF)

Deposit WMM7 was dominated by Fe, Ca, Cu and Ti. Elements likely to be indicative of minerogenic inputs (e.g. Ti, Al, K, Ca), for example from windblown particulates, had low signals overall (Figure D1). There were no horizons of elevated minerogenic inputs which might be expected during a hiatus in stomach-oil accumulation. Elements with both a biogenic and minerogenic (e.g. Cu, Fe) or principally biogenic source (e.g. As, Zn) (Huang et al., 2009; Liu et al., 2013) varied both at the mm-scale (likely reflecting individual laminae) and with depth in the deposit (Figure D1). To account for the influence of

minerogenic contributions to the elemental composition of WMM7, all data were normalised to Ti (Fig. 3, Figure DE1). There were no clear down-core trends in Fe/Ti and Si/Ti (Fig. 3a,b) indicating a dominant minerogenic source for Fe and Si. Cu/Ti was generally elevated 30.3-28.6 ka with minima ca. 29.3 ka (Unit III), and very low values between 28.5-27.4 ka (Unit II).
280 Highest Cu/Ti was recorded between 27.4-26.9 ka, then remained elevated until 25.7 ka (Unit I), until values decreased to the top of the deposit (Fig. 3c). Cu/Ti was high but showed a long-term decrease from the base of the deposit (28.8 ka) to 25.7 ka (Units III and II). High Cu/Ti was recorded between 25.7-24.0 ka (Unit I), then values decreased to the top of the deposit (Fig. 3c). In contrast, Br/Ti and S/Ti were low from 28.830.3 ka to 28.726.8 ka (Unit III), then elevated between 26.828.7-27.4-25.7 ka (Unit II; Fig. 3d,e). A gradual increase in Br/Ti and S/Ti was then recorded until a second maximum at 23.925.5 ka (Unit
285 I); both Br and S then decreased to 22.924.5 ka. A dominant biogenic source for the trends in Si, Cu, Br and S is inferred for WMM7, noting that the patterns in Br/Ti and S/Ti were different to those of Cu/Ti, and may include a sea-salt origin given some similarities to Cl/Ti (not shown; *r2*=0.36).

290
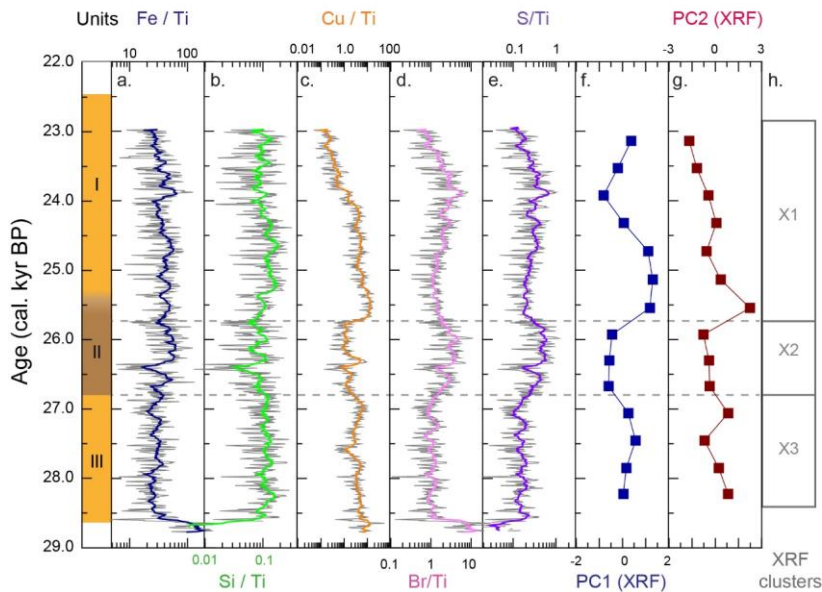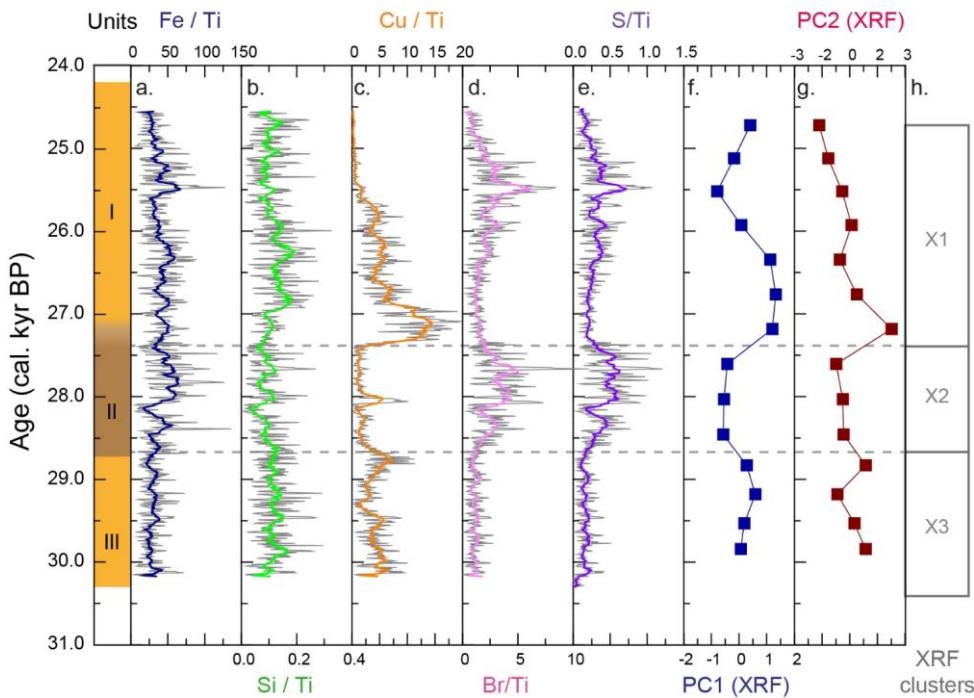
Figure 3: XRF characterisation of stomach-oil deposit WMM7. Age model uses Holocene "no sea ice" *ΔR* (Table 1). All XRF data normalised to Ti and on a log scale. ~100 yr smoothing in coloured lines. Cluster boundaries determined by constrained hierarchical clustering analysis in the *rioja* package of *R* (Juggins, 2020), compared to broken-stick analysis (Bennett, 1996). Three significant clusters were identified (h.), which broadly coincide with Units I-III, noting the gradual Unit II/I boundary.

The PCA of the XRF data confirms that there were two main patterns in the elemental composition of WMM7 (Fig. 3f,g; Table 2). PC1, which accounted for 93% of the variance, and driven by positive loading from Fe, Cu and Ca, which could have both minerogenic and biogenic origins. PC2 accounted for 6% of the variance, driven by Cu (positive loading), Ca and Fe (negative loading), but PC2 was not a statistically significant factor using the broken-stick threshold in PAST3. Peaks in PC1 occurred before 28.527.0 ka (Unit III), and between 27.1-26.3 ka (lower Unit I) and at 24.7 (uppermost Unit I)at 25.5 and 24.75 ka (lower Unit I). PC1 minima occurred in Unit II (28.5-27.6 ka26.75 26.0 ka) when high Br/Ti and S/Ti confirmed enhanced organic matter inputs. In contrast, PC2 broadly followed the Cu/Ti trend, recording declining values from 29.9-27.628.25 26.0

305   ka (Units III and II), and peak values at 27.1 25.25 ka (lower Unit Il, Fig. 3). Three clusters were identified in the re-sampled

XRF data (Fig. 3i), broadly aligned to Units I-III.

Table 2 Principal component analysis. The elements contributing to each principal component are shown; grey shading highlights Fe, Cu and Ca which dominate the loadings. PC1 explains 93% of the variance (statistically significant) whereas PC2 explains only
310   **6% of the variance and is not statistically significant. PC1 and PC2 through time are shown in Fig. 3.**

Principal component loadings	PC 1	PC 2
Si	0.003	0.001
P	0.001	-0.002
S	0.004	-0.009
Cl	0.013	-0.034
K	0.028	-0.051
Ca	0.162	-0.165
Ti	0.026	-0.019
Cr	0.004	-0.003
Mn	0.010	-0.006
Fe	0.961	-0.181
Cu	0.217	0.962
Zn	0.008	-0.005
Br	0.019	-0.008
Rb	0.002	-0.004
Sr	0.041	-0.091
Zr	0.009	-0.005

3.3 Organic matter composition

All WMM7 samples were highly organic-rich (27-50% C, 11-13% N, Figure EF1), with C/N ratios between 6 and 12 (Fig. 4a). The C/N ratios were consistent with high lipid and low N contributions as observed in modern Weddell Sea fish, bird and
315   seal tissues (Rau et al., 1992). The extracted lipids were dominated by fatty acids and alcohols (not presented here), consistent with the presence of triglycerides and wax esters observed today in stomach oils of procellariform seabirds i.e. albatrosses and petrels (e.g. Horgan and Barrett, 1985). The saturated fatty acids $C_{16:0}$ ($46 \pm 4\%$) and $C_{14:0}$ ($24 \pm 1\%$) dominated all samples, with additional minor contributions from $C_{18:1}$ ($16 \pm 3\%$), $C_{18:0}$ ($8 \pm 1\%$) and $C_{16:1}$ ($5 \pm 1\%$) (Fig. 4b,c).

320   The dominant fatty acids in WMM7 are consistent with a snow petrel diet of krill ($C_{14:0}$, $C_{16:0}$), squid ($C_{16:0}$) and fish ($C_{16:0}$, $C_{18:x}$) (Cripps et al., 1999; Lewis, 1966) (Table 3). To explore whether prey contributions changed through time, the relative

abundance of the major fatty acids were compared as ratios(Fig. 4d-f), assuming a krill ($C_{14:0}$), fish ($C_{18:x}$) or mixed source ($C_{16:0}$) (Table 3). Minor variations to $C_{18:0}/C_{16:0}$ occurred (0.18 ± 0.03, not shown), whereas $C_{18:0}/C_{18:1}$ broadly decreased from 30.3 to 25.9 ~~28.8 to 24.2~~ ka, then increased towards the top of the deposit (Fig. 4d). $C_{16:0}/C_{14:0}$ values were generally low

325   (~1.75) throughout the deposit, but peaked at 29.1-28.8 ka, 27.6 and 25.5 ka ~~27.25-27.0 ka, 25.75 and 23.75 ka~~. $C_{18:0}/C_{14:0}$ broadly increased from 27.4-25.9 ~~28.8-25.7~~ ka (Units III and II), decreased between 27.4-25.9 ~~25.7-24.2~~ ka (lower Unit I), then increased to reach a maximum at the top of the deposit (24.3 ~~22.6~~ ka).

330
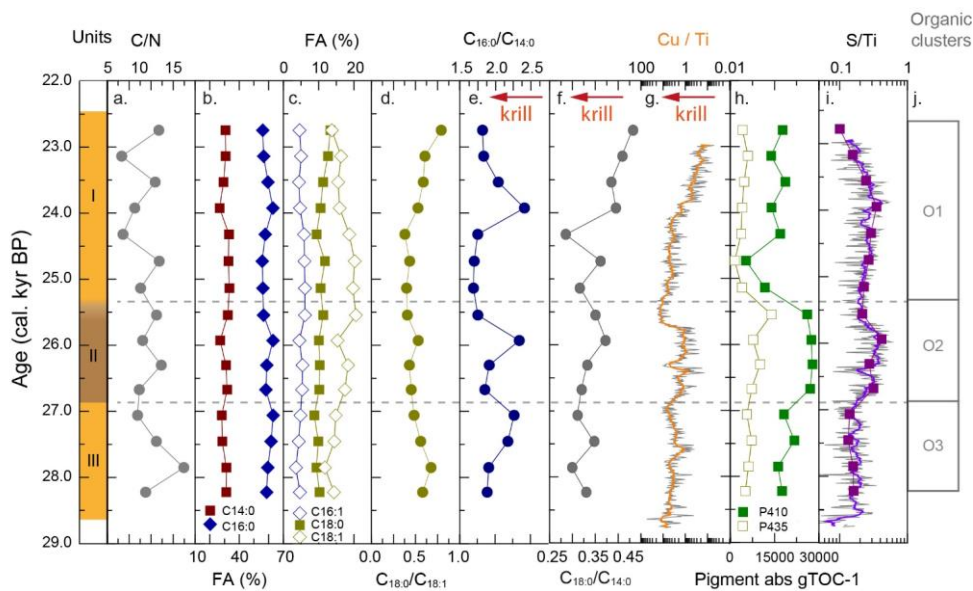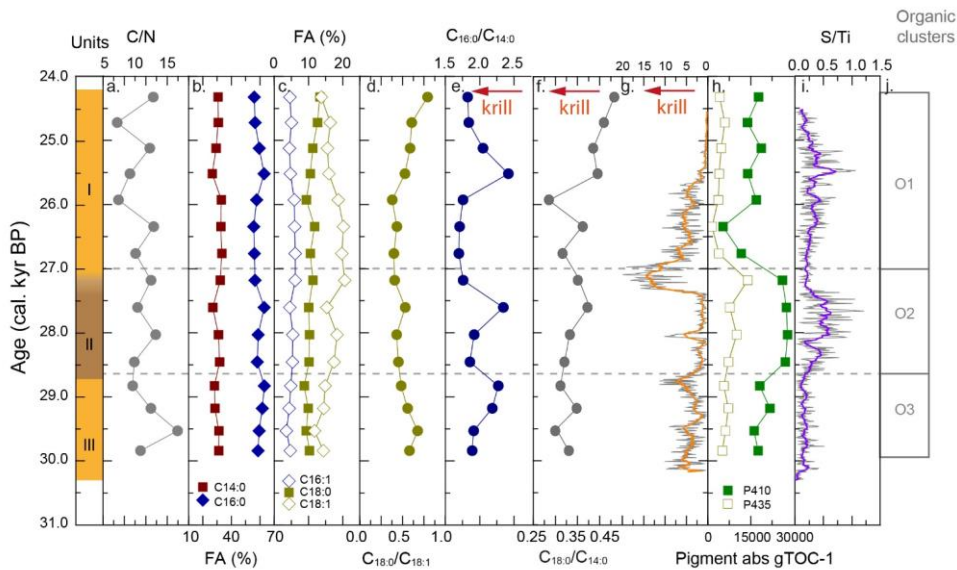
Figure 4: Organic matter composition of stomach-oil deposit WMM7. Age model uses Holocene "no sea ice" *ΔR* (Table 1). **Unit II highlighted with brown shading, noting gradual Unit II/I boundary. Cluster boundaries determined by constrained hierarchical clustering analysis in the *rioja* package of *R* (Juggins, 2020), compared to broken-stick analysis (Bennett, 1996). Three significant clusters were identified (j.), which broadly coincide with Units I-III, noting the gradual Unit II/I boundary. The Cu/Ti data from**

335 **Fig. 3 is shown in (g.), noting the reverse x-axis to align with the interpretation fatty acid indicators of krill in (e.) and (f.).**

The major pigments in WMM7 were P410 and P435 (Fig. 4h), consistent with chlorophyll derivatives ("chlorins"; (Harris and Maxwell, 1995)) and some carotenoid sources (Jeffrey et al., 1997). P665 nm, recording exclusively chlorins, was very low (3

340 orders of magnitude below P410, Figure ~~FE~~1). P410 was elevated 29.8-28.8 ka (Unit III) and showed a sustained maximum between 28.5-27.2 ka ~~P410 showed a sustained maximum between 28.7-25.5~~ (extending across the Unit II/I boundary, Fig. 4h). P435 remained low from the base of the sequence until a small peak at 27.2 ~~25.5~~ ka. A rapid decrease in P410 and P435 resulted in pigment minima at 26.3~~25.1~~ ka. From 25.9-24.3 ~~24.3-22.6~~ ka, P410 oscillated at intermediate values and there is a slight increase in P435 (Fig. 4h).

345

Table 3 Examples of snow petrel prey biochemistry, and oceanographic conditions related to snow petrel diet and prey distributions. Snow petrels forage in close association with the sea ice, either at the sea-ice edge or in leads or polynyas within the sea ice pack. The prey biochemistry information is used as a framework to interpret the chemical signatures recorded in stomach-oil deposit WMM7, including our use of fatty acid ratios to assess relative contributions of prey (Figs 4 and 5).

Environment	Characteristics	Expected signal recorded in stomach oil deposit and interpretation made here	References for prey biochemistry
Open ocean (pelagic)	Mixed snow petrel diet: krill, squid and fish. Krill species: _E. superba_ (Antarctic krill).	$C_{14:0}$, $C_{16:0}$, $C_{18:0}$ fatty acids and Cu (krill). $C_{16:0}$ fatty acids (squid). $C_{18:0}$ and $C_{18:1}$ fatty acids (fish). $\Rightarrow$ low $C_{16:0}/C_{14:0}$ (more krill) $\Rightarrow$ low $C_{18:0}/C_{14:0}$ (more krill) $\Rightarrow$ high Cu (more krill)	Cripps et al. (1999); Lewis, 1966); Rainbow (1989); Palmer et al. (1995); Liu et al. (2013)
Continental shelf (neritic)	More fish in snow petrel diet. Potential for krill to include _Euphausia crystallorophias_ (ice krill) as well as _E. superba_.	Increased $C_{18:0}$ and $C_{18:1}$ fatty acids $\Rightarrow$ high $C_{16:0}/C_{14:0}$ (less krill) $\Rightarrow$ high $C_{18:0}/C_{14:0}$ (less krill) $\Rightarrow$ low Cu (less krill)	Bottino 91975) ; Imber (1976); Raclot et al. (1998); Mayzaud et al. (2011) ; Ju and Harvey (2004).

350

3.4 Stable isotope composition

Bulk $\delta^{13}C$ ranged from -27.0 to -29.9 ‰. Bulk $\delta^{15}N$ ranged between 11.1 to 12.6 ‰. There was a positive correlation between $\delta^{15}N_{bulk}$ and $\delta^{13}C_{bulk}$ between 30.3-25.9 28.8-24.3 ka, but they were negatively correlated after 25.9 24.3 ka (Fig. 5a,b). The two major fatty acids were offset from $\delta^{13}C_{bulk}$ by up to -5.8‰ (-3.3 ± 1.4‰, $C_{14:0}$) and up to -3.9‰ (-1.3 ± 1.6 ‰, $C_{16:0}$; Fig. 5c). The most enriched values were recorded by $\delta^{13}C_{18:1}$ (-26.0 ± 1.2 ‰), which is offset to $\delta^{13}C_{18:0}$ by +1.27 ± 1.3 ‰, and to $\delta^{13}C_{bulk}$ by +2.1 ± 1.6 ‰. Although lipid $\delta^{13}C$ is usually depleted relative to $\delta^{13}C_{bulk}$ as a result of fractionation during lipid synthesis (e.g. Rau et al., 1992), the dominance of lipids in WMM7 resulted in $\delta^{13}C_{bulk}$ reflecting the combined influences of the main lipid components.

Fatty acid $\delta^{13}C$ showed several short-term oscillations (Fig. 5c). Both $\delta^{13}C_{16:0}$ and $\delta^{13}C_{14:0}$ decreased from 29.4-28.4 27.9-26.3 ka (Unit III, lower Unit II) whereas $\delta^{13}C_{18:0}$ increased and $\delta^{13}C_{18:1}$ showed no clear trend. All fatty acid $\delta^{13}C$ were low at 28.4 26.3 ka (Unit II). The $\delta^{13}C_{14:0}$ remained low from 28.4-27.4 26.3-25.7 ka (Unit II), whereas $\delta^{13}C_{16:0}$ and $\delta^{13}C_{18:0}$ increased until 26.7 25.1 and 27.1 25.5 ka, respectively (Unit I). Unit I showed highly variable fatty acid $\delta^{13}C$. Minima in $\delta^{13}C_{14:0}$ and $\delta^{13}C_{18:0}$ were recorded at 26.7 25.1 ka, and subsequently in $\delta^{13}C_{16:0}$ and $\delta^{13}C_{18:1}$ at 26.2 24.7 ka. All fatty acid $\delta^{13}C$ increased to 25.4 24.0 ka and showed a slight decrease at the top sample (25.0 23.5 ka). The relationships between the four fatty acid $\delta^{13}C$ changed through time: from 29.4-28.4 27.9-26.7 ka there was a close relationship between $\delta^{13}C_{14:0}$ and $\delta^{13}C_{16:0}$. In contrast, from 28.4 26.7 ka the $\delta^{13}C_{14:0}$ correlated with $\delta^{13}C_{18:0}$, and $\delta^{13}C_{16:0}$ with $\delta^{13}C_{18:1}$.

Cluster analysis on the lipids, pigments and stable isotope data identified 3 zones (Fig. 4j, Figure C1). The lower zones aligned with Units III and II, but the upper zone boundary occurred at ~25.3 27.0 ka, slightly above the Unit II/I and XRF zone boundaries and likely driven by the sustained maxima in P410 (Fig. 4h).
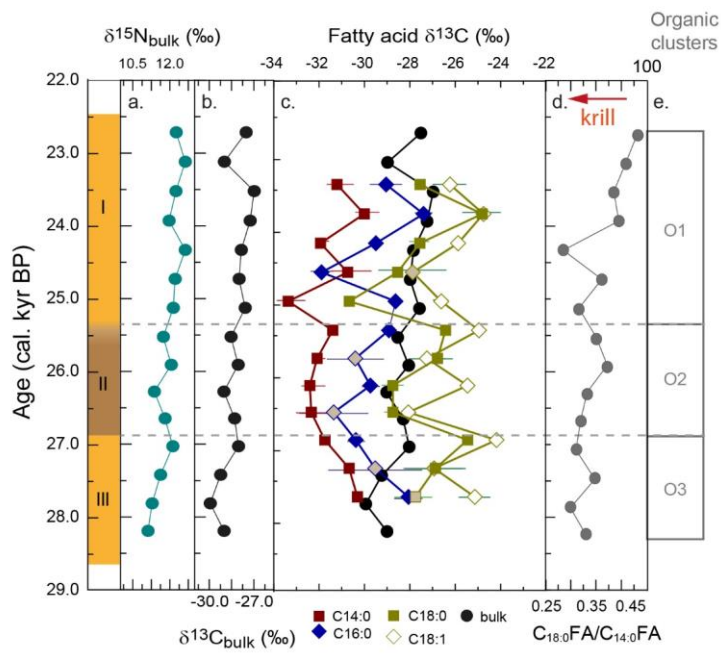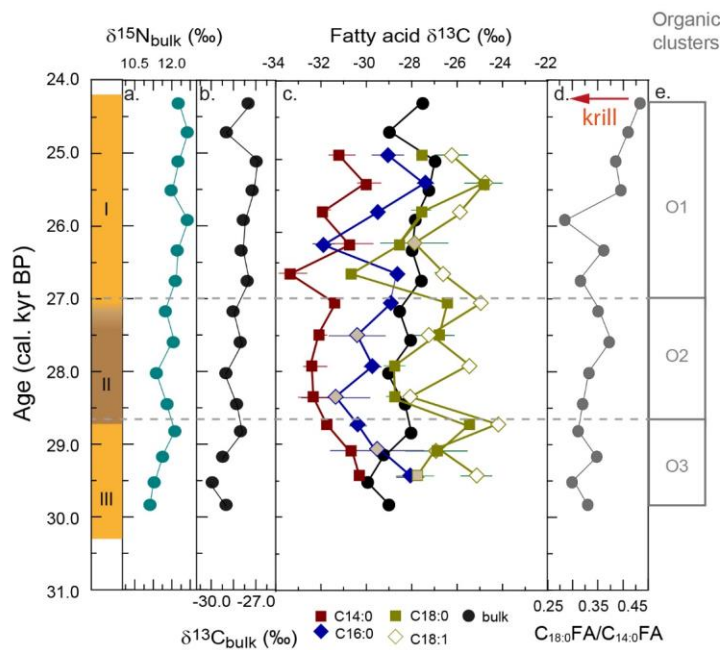
375 **Figure 5: Stable isotope ratios in organic matter from stomach-oil deposit WMM7. Age model uses Holocene "no sea ice" _ΔR_ (Table 1). (a.) bulk $\delta^{15}N$; (b.) bulk $\delta^{13}C$; (c) fatty acid $\delta^{13}C$ and bulk $\delta^{13}C$. Standard deviation of replicates are shown: where no error bar is visible the standard variation is smaller than the width of the symbol. Grey shaded data points are those for which the standard variation of the repeat measurements indicated poor reproducibility (>1 ‰). (d.) $C_{18:0}/C_{14:0}$ fatty acid ratio as an indication of relative krill contribution, from Fig. 4; (e.) cluster boundaries from Fig. 4.**

380

4 Discussion

Stomach-oil deposit WMM7 is characterised by biochemical variability which can be attributed to changing biogenic composition through time. In this section, we first evaluate the likely sources of this variation, infer changes in snow petrel diet through time, and investigate how the sea-ice environment may have varied. By doing this we aim to provide greater

385 insight both into the biochemistry of the stomach-oil deposit, and into critically evaluating its use as a palaeo-environmental archive.

4.1 Contributions to stomach-oil biochemistry

The stomach oil regurgitated by snow petrels at nesting sites provide an integrated archive of diet during the most recent foraging trip in the summer breeding season. These trips may be for several days (Barbraud et al., 1999). During this time, the snow petrel concentrates the lipid components of their prey into stomach oil; this provides an energy-rich food source for their chicks (Warham, 1977; Watts and Warham, 1976), and can be spat in defence against predators, or against other snow petrels in disputes over access to suitable crevices for nesting. Unlike muscle, feather or adipose tissues, which involve biosynthesis (e.g. Rau et al., 1992), the basic biochemical composition of the prey is not altered during stomach oil formation (Watts and Warham, 1976). Thus, the stomach-oil deposits provide a window into the biochemistry of the prey consumed by snow petrels in open waters at the margins of, or within, the sea-ice zone.

We have considered non-diet influences on the stomach-oil deposit geochemistry. A contribution of snow petrel guano to stomach-oil deposits has been indicated previously (Berg et al., 2019; Hiller et al., 1988). However, WMM7 does not show the negative relationship between C/N and other elements (Cl, P, S) which would have been expected if there was a strong residual signature of guano contributions to the deposits (Berg et al., 2019). The C/N ratios are consistent with particulate organic carbon (~10) in modern sea ice (Henley et al., 2012) and fish collected in the Weddell and Lazarev Seas (~3-11) (Rau et al., 1992; Friedrich and Hagen, 1994). We suggest that any contribution of guano to WMM7 is lower than for other published sequences derived from DML stomach-oil deposits (Berg et al., 2019), perhaps due to local topography (including aspect and microclimate), the distance from the nest that the sample was taken, or the history of occupation.

We did not observe formation of K- and C-bearing phosphates by weathering (Berg et al., 2019); rather, the highest P counts were recorded in Unit II where Ca counts were lower and there was no change in K (Figure BA1). Progressive oxidation of organic matter was not evident: no systematic trends in labile pigment abundances (Fig. 4h) nor fatty acid δ^{13}C were observed (Fig. 5). Furthermore, bulk δ^{13}C are negatively correlated to C/N, as observed today in Antarctic fish (and other predators), reflecting the variable contributions of ^{13}C-depleted and low N lipids to the bulk signal (Rau et al., 1992; Friedrich and Hagen, 1994; Cherel et al., 2011). Again, this difference in weathering signal between deposits may reflect local factors at the nesting sites (discussed above).

As observed in other glacial-stage stomach-oil deposits (Berg et al., 2019), WMM7 differs from some modern snow petrel stomach oils (e.g. Warham et al., 1976) by substantially lower contributions of $C_{18:1}$ relative to $C_{16:0}$ and $C_{14:0}$. The lower contributions of polyunsaturated (<1%) and monounsaturated fatty acids (e.g. $C_{18:1}$ 9 ± 2%, $C_{16:1}$ 2.6 ± 0.3%) than in fresh stomach oil of other procellariiform seabirds (Connan et al., 2007) including snow petrels (Warham et al., 1976; Watts and Warham, 1976) could indicate post-depositional oxidation (Berg et al., 2019). However, similar fatty acid contributions to WMM7 have been recorded in a late Holocene DML stomach-oil deposit (Aiello et al., 2011), in prey of snow petrels (Cripps

420 et al., 1999) and in stomach oils from other Procellariiformes (Wang et al., 2007). As previously noted (Berg et al., 2019), the samples of fresh stomach oils (Warham et al., 1976; Watts and Warham, 1976) were from snow petrels foraging in the Ross Sea, where prey availability, and hence stomach oil biochemistry, may also be different. We therefore suggest that the fatty acid signatures in WMM7 primarily signal a dietary intake, rather than variable preservation.

425 Analyses of stomach contents and observations at sea indicate that snow petrel diet is dominated by fish (12-95%) and krill (35-71%) (e.g. Ridoux and Offredo, 1989; Ainley et al., 1984; Falla, 1937; Fijn et al., 2012), including the Antarctic silverfish *Pleuragramma antarctica* (Family: Nototheniidae) and Antarctic lanternfish *Electrona antarctica* (Family: Myctophidae) (Ainley et al., 2006; Ainley et al., 1984). Variable contributions from squid have also been recorded (Ridoux and Offredo, 1989; Ainley et al., 1984; Bierman and Voous, 1950). The dominant fatty acids in WMM7 are consistent with the main snow

430 petrel prey (Table 3): Antarctic krill (*Euphausia superba*, high abundances of $C_{14:0}$, $C_{16:0}$, sometimes $C_{18:1}$ (Cripps et al., 1999; Raclot et al., 1998)), squid (dominated by $C_{16:0}$, plus longer-chain fatty acids $C_{20:5}$ and $C_{22:6}$)(Raclot et al., 1998)), and both notothenoid and myctophid fish (high concentrations of $C_{18:1(n-9)}$, $C_{16:0}$, and several mono- and poly-unsaturated C_{20} and C_{22} fatty acids (Imber, 1976; Raclot et al., 1998; Mayzaud et al., 2011)). Although only recorded as a minor (~2%) contributor to snow petrel diet (Ridoux and Offredo, 1989), in coastal waters ice krill (*Euphausia crystallorophias*) is found in very high

435 densities (La et al., 2015), characterised by high abundances of the $C_{18:1\omega9}$ and $C_{16:0}$ fatty acids as well as $C_{14:0}$ and $C_{16:0}$ alcohols (Ju and Harvey, 2004; Bottino, 1975). The $C_{16:0}$ thus has a mixed origin from krill, fish and squid in contrast to $C_{14:0}$ (Antarctic krill) and $C_{18:x}$ (fish). The offsets in $\delta^{13}C$ for $C_{14:0}$, $C_{16:0}$ and $C_{18:x}$ (and their different trends through time) confirm that they have different sources in WMM7 (Fig. 5). The offsets between individual fatty acids exceeds the ~1‰ enrichment which might be expected through an increase in trophic level (Post, 2002), suggesting an alternative control through temporal or spatial

440 variations in foraging habitat of the snow petrels and/or their prey (Section 4.3).

Our interpretation of $C_{14:0}$ as an indicator of Antarctic krill inputs to snow petrel diet is broadly supported by elevated Cu (measured as Cu/Ti) (Rainbow, 1989; Palmer Locarnini and Presley, 1995; Liu et al., 2013) when $C_{14:0}$ is also relatively high (by $C_{16:0}/C_{14:0}$ and $C_{18:0}/C_{14:0}$)(Fig. 4). Thus, we here identify two independent measures of the relative contributions of krill

445 which can be applied to WMM7 to investigate broad-scale changes in snow petrel diet through time.

4.2 Snow petrel diet 30.3-24.3 28.8-22.6 ka

The variation in biogenic contributions to stomach-oil deposit WMM7 reveal changing snow petrel diet at decadal (XRF data), centennial and millennial timescales, for the early part of Marine Isotope Stage (MIS) 2, which includes the start of the LGM (30.3-24.3 28.8-22.6 ka). We note that although each stomach oil regurgitation provides a snapshot of snow petrel diet during

450 the summer breeding season (November to February), prey biochemistry (and thus stomach oil composition) may also provide information over varying timescales, reflecting lifecycle and tissue turnover rates of the fish, krill and squid consumed by the snow petrel.

Our multi-proxy analysis confirmed that three zones could be identified. Between 30.3-28.7 ~~28.8-26.8~~ ka (~Unit III) elevated Cu/Ti and $C_{14:0}$ contributions (low $C_{16:0}/C_{14:0}$ and $C_{18:0}/C_{14:0}$) identified Antarctic krill as an important component of snow petrel diet, but likely decreasing through time. Although offset by ~2.0‰, supporting different sources, both $\delta^{13}C_{14:0}$ and $\delta^{13}C_{16:0}$ decreased across this time interval, suggesting either a common environmental (prey habitat) signal or that Antarctic krill contributed to both $C_{14:0}$ and $C_{16:0}$. In contrast, the much higher (and increasing) $\delta^{13}C_{18:0}$ and $\delta^{13}C_{18:1}$ confirmed a different prey source and/or habitat signal contributing to the C_{18} fatty acids. Thus, the prey other than Antarctic krill, which were most likely to be fish, occupied a different foraging habitat (see Sect. 4.3).

At 28.7 ~~26.8~~ ka (Unit II) there was a shift in the dominant contributions to the snow petrel stomach oils. Low Cu/Ti and increasing $C_{16:0}/C_{14:0}$ and $C_{18:0}/C_{14:0}$ indicate a prolonged (~1100 yr) interval where Antarctic krill was not a major component of snow petrel diet (Figs 3,4). Reduced minerogenic inputs (Fig. 3f) and increased marine organic matter (Figs 4h,i) characterise Unit II: low PC1, elevated S, Br (e.g. Leri et al., 2010), chlorins, and $C_{18:1}$ (Jónasdóttir, 2019; Cripps et al., 1999). Although this biochemical signature suggests a dominant phytoplankton fingerprint in snow petrel diet between 28.5-27.2 ~~26.8-24.7~~ ka, phytoplankton are too small to be consumed directly by seabirds. The elevated chlorins (Fig. 4h) seem more likely to indicate the snow petrels consumed prey with a phytoplankton-dominated diet. Decreasing $\delta^{15}N_{bulk}$ in Unit II may also reflect a shorter food-chain, although the shift is small (<1‰, Fig. 5). Preservation of intact phytoplankton in stomach oils is also feasible through secondary ingestion (i.e. in the stomachs of snow petrel prey), since undigested algal cells have been reported in penguin guano (Mychra and Tatur, 1991) and diatoms have been isolated in *P. antarctica* larvae (Vallet et al., 2011) and other stomach-oil deposits (Berg et al., 2019).

The similarity in the trends between $\delta^{13}C_{16:0}$ and $\delta^{13}C_{18:1}$ (Fig. 5c) confirms an increased importance of prey with C_{18} fatty acids in their tissues between 28.7-27.2 ~~26.8-24.7~~ ka, consistent with incorporation of a phytoplankton signal in predator tissues, through their consumption of copepods, squid or fish, which can occur with minimal alteration (e.g. Lee et al., 1971). Elevated (~20%) $C_{18:1}$ through Units I and II supports an increased contribution of fish to the snow petrel diet between 28.7-27.4 ~~26.8-25.7~~ ka, but identifying the particular fish species is more challenging. Both *P. antarctica* (Mayzaud et al., 2011) and several species of myctophid fish including *E. antarctica* (Imber, 1976; Raclot et al., 1998) contain $C_{18:1}$, and their $\delta^{13}C$ and $\delta^{15}N$ values suggest that *P. antarctica* and *E. antarctica* have overlapping trophic niches (Rau et al., 1992). High abundances of $C_{16:0}$ in myctophids (Mayzaud et al., 2011) may account for the similarity in $\delta^{13}C_{16:0}$ and $\delta^{13}C_{18:1}$ in Unit II. Although the main myctophid prey today are euphausiids (including krill, (Saunders et al., 2019)), this diet is not consistent with the low Cu/Ti and low $C_{14:0}$ contributions to WMM7 in Unit II, nor with the >4‰ offset between $\delta^{13}C_{14:0}$ and $\delta^{13}C_{18:1}$. Alternatively, an increased contribution from nototheniid fish (e.g. *P. antarctica*), the diet of which includes copepods as well as krill, might

explain the apparently elevated phytoplankton signature and the reduced contribution of krill to snow petrel diet throughout Unit II.

From 27.4-25.9 25.7-24.2 ka (lower Unit I), Antarctic krill returned as an important component (high Cu/Ti, higher $C_{14:0}$ contributions), although the positive relationship between $\delta^{13}C_{16:0}$ and $\delta^{13}C_{18:1}$ suggests that fish was also important in the diet. Reduced input of marine organic matter was apparent in Br, S and chlorins (Figs 3 and 4). Fatty acids $\delta^{13}C$ showed higher variability than in Units II and III. From 25.2 24.2 ka to the top of the deposit (22.6 24.3 ka; Upper Unit I), increasing minerogenic contributions may explain the simultaneous decrease in Cu/Ti, Br/Ti and S/Ti, which contrasts with the anti-phase behaviour between Cu and Br or S discussed previously, and for the Cu/Ti minima whilst $C_{14:0}$ inputs increase slightly. Fatty acids $\delta^{13}C$ also show concomitant peaks and lows from 25.5-25.0 ka fluctuate in parallel from 24.2-23.5 ka, suggesting there may be a strong baseline (i.e. primary producer) control over the stable isotope values.

We note that the changes in relative contributions of Antarctic krill and fish in the diet that we inferred for WMM7 are not reflected in the range of $\delta^{15}N_{bulk}$ (~1.2‰), which lies below modern trophic level offsets of >2 ‰ (e.g. Seyboth et al., 2018) including some krill-fish offsets of ~5-7 ‰ in the Southern Ocean (e.g. Polito et al., 2011), and suggests minimal changes to snow petrel trophic level between 30.3-24.3 28.8-22.6 ka. However, $\delta^{15}N_{bulk}$ reflects $\delta^{15}N$ in prey tissues which can themselves vary over space and time (Quillfeldt and Masello, 2020), so that trophic values can only be calculated if baseline (primary producer) $\delta^{15}N$ is known (Post, 2002). Since baseline $\delta^{15}N$ is poorly constrained for our interval of study, and since snow petrel prey integrate $\delta^{15}N$ across different temporal and spatial scales, it seems likely that the small range of $\delta^{15}N_{bulk}$ in WMM7 reflects either baseline $\delta^{15}N_{bulk}$ or mixing of multiple signals over time, which we are unable to disentangle with our analyses.

In summary, the stomach-oil deposit WMM7 indicates several changes to snow petrel diet between 30.3 and 24.3 28.8 and 22.6 ka. Antarctic Kkrill and fish provided important contributions between 30.3-28.7 28.8-26.8 ka (Unit III) and 27.4-24.3 25.7-22.6 ka (Unit I). Between 28.7-27.4 26.8-25.7 ka (Unit II) a prolonged interval of low krill contributions suggests a shift towards a more fish-dominated diet. The strong phytoplankton fingerprint during this time also suggests that the fish themselves had a reduced krill contribution to their diet, highlighting a substantial change to the food chain in the foraging habitat of the snow petrels. In the following section, we consider the likely palaeo-environmental drivers and implications of these signals.

4.3 Evolution of sea-ice environments (30.3-24.3 28.8-22.6 ka)

Seabird diets vary over time and space, depending on the availability of prey species, in turn reflecting environmental conditions within their foraging range (Mills et al., 2020; Mills et al., 2021). For example, it has been proposed that myctophid fish become more important to seabird diet when krill availability is low, during winter when sea ice is more extensive and/or

in response to temporal and spatial changes in summer production (Nicol, 2006; Watanuki and Thiebot, 2018). Prey biochemistry may also reveal environmental information: $\delta^{13}C$ decreases with increasing latitude (Francois et al., 1993; Trull and Armand, 2001) or between coastal and offshore waters (Trull and Armand, 2001), whereas $\delta^{13}C$ increases within the sea

520 ice during spring melt (Dunbar and Leventer, 1992). These differences are reflected in the $\delta^{13}C$ of crustaceans, fish and squid in these habitats, and in turn in their predators including seabirds (Cherel et al., 2011; Jaeger and Cherel, 2011; Delord et al., 2016; Phillips et al., 2009).

The presence of multiple stomach-oil deposits in DML during MIS 3 and the early LGM (Berg et al., 2019) confirms that there
525 must have been accessible prey within range of the breeding snow petrels at Lake Untersee during the spring and summer. WMM7 has a very stable accumulation rate (Fig. 2) and we found no evidence for hiatuses, suggesting that the site was not affected by long periods of nest-site abandonment related to unfavourable climatic conditions (e.g. snow cover over the site, perennial sea ice preventing access to prey within foraging range) or local factors (e.g. burial by rock) (Olivier and Wotherspoon, 2006; Olivier et al., 2005). We consider it unlikely that the snow petrels were foraging at an oscillating
530 spring/summer sea-ice margin, because WMM7 deposition coincides with an expanding then maximum summer sea–ice extent in the Atlantic sector of the Southern Ocean between 29-22 ka (Fig. 6) (Collins et al., 2012; Gersonde et al., 2005; Gersonde et al., 2003; Allen et al., 2011; Fischer et al., 2007; Xiao et al., 2016; Goto-Azuma et al., 2019), which places the summer sea-ice margin at 55-60°S, >1500-2000 km away from WMM7 and far beyond the typical maximum foraging range for this species (Fig. 1).

535

Today, snow petrel foraging in high (>80%) sea-ice concentrations occurs in the margins of polynyas (Ainley et al., 1984), regions of open water within the winter- or multi-year sea-ice pack, which are critical for enabling high levels of primary productivity, carbon cycling and air-sea gas exchange (Arrigo et al., 2008; Sherrell et al., 2015). Several marine sites in the Weddell and Lazarev Seas have indicated sporadic polynya formation during MIS 2 and 3 (Fig. 1) (Sprenk et al., 2014; Smith
540 et al., 2010; Thatje et al., 2008; Weber et al., 1994). Deposit WMM7 confirms previous proposals that polynyas were important for supporting snow petrel colonies through the last glacial (Thatje et al., 2008; Berg et al., 2019). We interpret our new records of changes in snow petrel diet in MIS 2 to have occurred as a result of changes to conditions within, and/or the locations of, polynyas offshore of DML. Unlike today, where polynyas are largely winter/spring phenomena which impact spring-summer productivity during or after sea-ice melt as "post polynyas" (Arrigo and van Dijken, 2003), summer sea surface temperatures
545 below freezing in the Weddell Sea (Gersonde et al., 2005) would have supported more extensive sea ice (and polynya) formation in summer during the last glacial stage (Fischer et al., 2007).
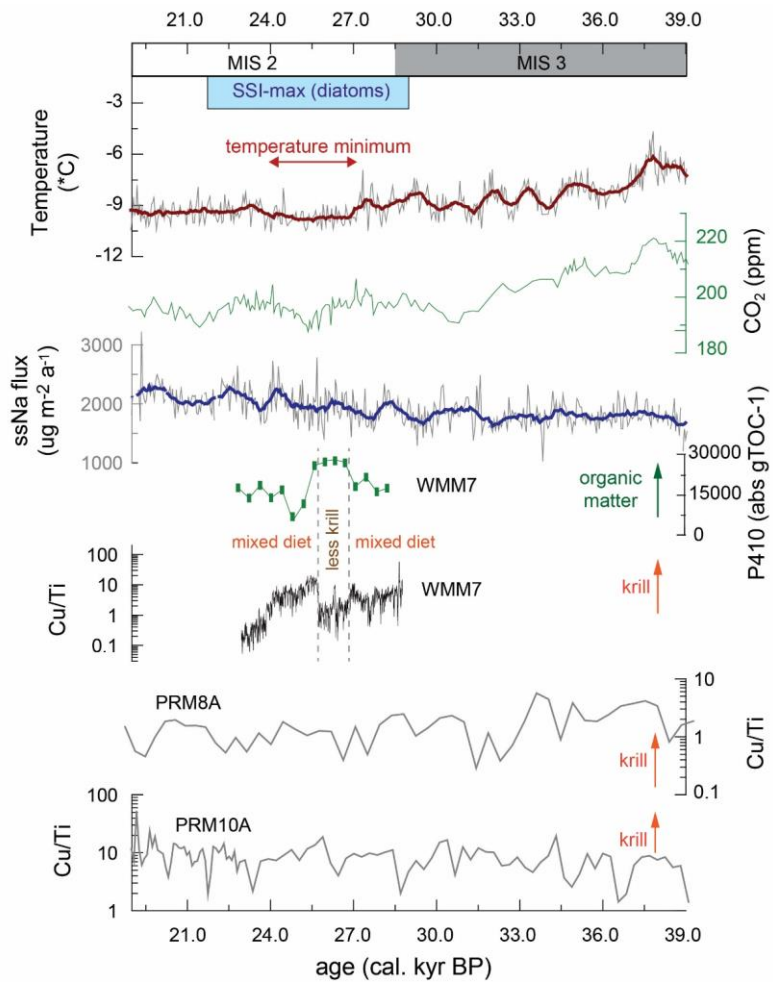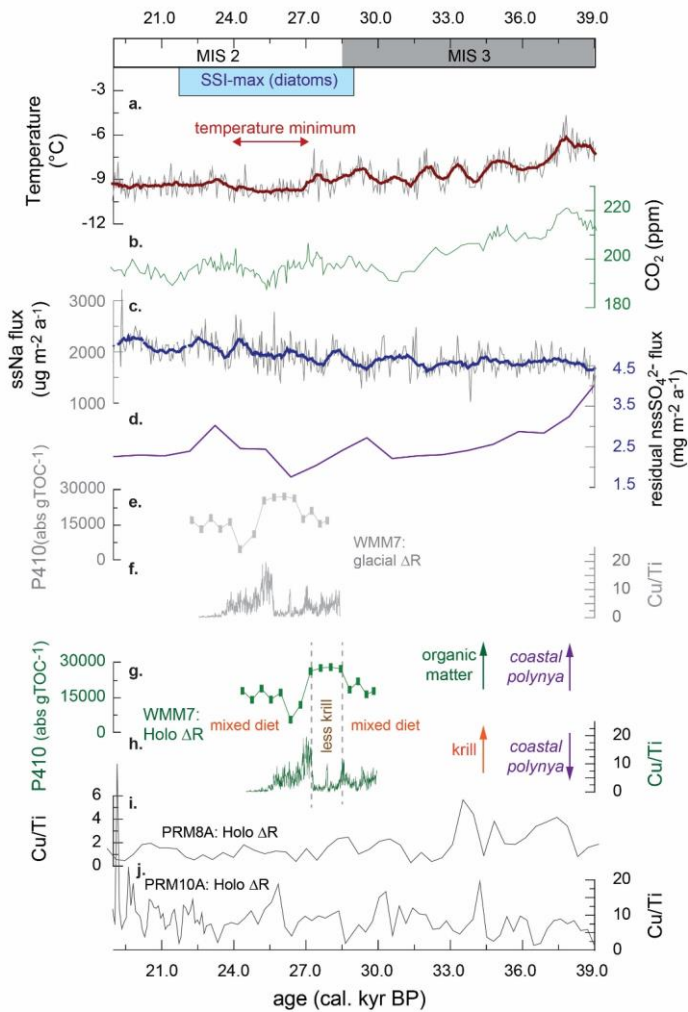
550 **Figure 6: variations in snow petrel diet across the MIS 3-2 transition, including the interval of maximum summer sea-ice extent (SSI-max) in the Scotia Sea from Allen et al. (2011) and plotted in Fig.1. (a.) air temperature recorded by δD in EPICA-DML ice core (Jouzel et al., 2007); (b.) atmospheric CO₂ from West Antarctic Ice Sheet (WAIS) ice core (Bauska et al., 2021); (c) sea-salt Na flux from EPICA-DML ice core (Fischer et al., 2007); ((d.) biogenic sulphate flux to EPICA-DML ice core, generated by correcting for terrestrial contributions to non-sea salt Na flux (Goto-Azuma et al., 2019); (e.) WMM7 chlorin pigment abundance plotted using**

Diet studies in recent decades indicate that snow petrels consume a mixed diet of krill, squid and myctophid fish when feeding beyond the continental shelf, whereas fish are most important in shelf waters, at least in the Ross Sea (Ainley et al., 1992; Fijn et al., 2012; e.g. Ridoux and Offredo, 1989; Ainley et al., 1984; Falla, 1937). A similar pattern in Antarctic petrels (*Thalassoica antarctica*) has been attributed to a lack of Antarctic krill inshore during the breeding season (Nicol, 1993). Although adult krill and larvae over-winter within the sea ice, post-larval krill are mostly oceanic (Atkinson et al., 2008). During the austral spring and summer, corresponding to the breeding season of the snow petrels, adult krill move to deeper waters for egg development (Nicol, 2006), which may account for the observed increase in krill in snow petrel diets when they forage beyond the continental shelf. Given the importance of deep waters for the Antarctic krill lifecycle, we infer that the mixed diet of krill and fish in Units I and III represent snow petrels foraging in polynyas located beyond the continental shelf. In contrast, the observed shift in fatty acid and element profiles in Unit II suggests that fish became more important to snow petrel diet, suggesting that polynyas had opened up over the continental shelf between 28.7-27.4 26.8-25.7 ka. We hypothesise that these shifts in foraging habitat reflect changes in sea ice conditions, by either influencing prey distributions or access to surface waters for feeding.

We discount a latitudinal control over $\delta^{13}C$ in WMM7, because the seasonal and spatial ranges of $\delta^{13}C$ within sea ice can exceed the Southern Ocean latitudinal $\delta^{13}C$ gradient (Dunbar and Leventer, 1992; Kennedy et al., 2002) due to changing $CO_{2(aq)}$ supply and productivity (Henley et al., 2012; Kennedy et al., 2002). Organic matter in the sea-ice zone tends to have elevated $\delta^{13}C$ compared to open waters beyond the ice edge (Henley et al., 2012; Kennedy et al., 2002), but $\delta^{13}C_{14:0}$ production in open waters for WMM7 is not consistent with the expanded sea ice extent of MIS 3-2 outlined above. Rather, low $\delta^{13}C_{14:0}$ is consistent with (krill) production in the winter/spring sea ice (Dunbar and Leventer, 1992; Henley et al., 2012) and/or more oceanic (rather than coastal) habitats (Cherel et al., 2011), with ^{13}C-enriched C_{18} fatty acids in WMM7 reflecting primary production and fish tissues from summer and/or more coastal habitats. No long-term trends are recorded in $\delta^{13}C_{18:0}$ or $\delta^{13}C_{18:1}$, and all four of the major fatty acids have highly variable $\delta^{13}C$ (ranges >2‰) after 25.327.0 ka (Unit I). In contrast, a long-term decrease in $\delta^{13}C_{14:0}$ between 29.4-28.4 27.9-26.3 ka (Units III and II) occurs alongside declining Antarctic krill contributions

(Cu/Ti and $C_{18:0}/C_{14:0}$). The cause of the long-term decline in $\delta^{13}C_{14:0}$ is unclear, but could reflect prolonged winter (low $\delta^{13}C$) sea ice, which leads to ^{13}C-depletion (Dunbar and Leventer, 1992) and also to restricted access to krill (Watanabe et al., 2020), even though increased winter sea ice is important for Antarctic krill recruitment (Atkinson et al., 2004; Jaeger and Cherel, 2011). Alternatively, declining $\delta^{13}C_{14:0}$ could reflect enhanced upwelling of $CO_{2(aq)}$ rich waters but low $\delta^{13}C$ circumpolar deep water (Bostock et al., 2004; Menviel et al., 2015) during the season of krill production. The decreasing $\delta^{13}C_{14:0}$ and krill contributions from 28.830.3 ka culminate in the shift to a diet rich in fish by 26.828.7 ka (Unit II) which we infer to represent coastal polynya development, reducing krill recruitment in shallower waters and/or reducing snow petrel access to krill with more widespread spring sea ice. Elevated phytoplankton contributions between 28.5-27.2 25.5-24.7 ka in WMM7 are also consistent with the highest primary productivity and/or low grazing observed today in shallow (continental shelf) waters, including coastal polynyas (Delmont et al., 2014; Karnovsky et al., 2007; Arrigo and van Dijken, 2003).

The cause of the millennial-scale switching between foraging in coastal and open-ocean polynyas is not clear, but could reflect ocean temperatures, wind speeds and directions (Morales Maqueda et al., 2004) and availability of continental shelf waters. Colder Southern Ocean waters during glacial stages (Gersonde et al., 2005) are expected to limit formation of those open-ocean polynyas which rely on ocean-driven sea ice melt (Ferrari et al., 2014) and reduced vertical mixing may have resulted from sea-ice driven stratification in the upper water column (Crosta and Shemesh, 2002). However, upwelling driven by wind and/or terraces on the continental slope may explain LGM polynya formation at site PS1506 (Thatje et al., 2008) and upstream of site PS1795 (Sprenk et al., 2014), within the foraging range of snow petrels breeding at Lake Untersee (Fig. 1). Enhanced wind speeds during glacial stages are also expected to have encouraged sea-ice break up and coastal (ice sheet- or ice shelf-proximal) polynya formation (Morales Maqueda and Rahmstorf, 2002; Sprenk et al., 2014; Smith et al., 2010; Weber et al., 1994), as observed today (Morales Maqueda et al., 2004).

Unlike other parts of the Antarctic ice sheet (Bentley et al., 2014), access of snow petrels to continental shelf waters during MIS 2 may also have been facilitated by relatively minor changes to vertical and lateral ice-sheet extent in DML over the last 100,000 years (Mackintosh et al., 2014; Hillenbrand et al., 2014). The exact position of the LGM ice-sheet limit on the DML continental shelf is not well constrained (Fig. 1)(Mackintosh Hillenbrand et al., 2014), but our data from WMM7 suggests that at least part of the continental shelf was free of glacial ice, enabling the development of coastal polynyas within MIS 2. Times of ice-sheet advance may then have reduced the area of available continental shelf and increased wind-driven polynya formation over the continental slope, as suggested by Weber *et al.* (1994) and Sprenk *et al.* (2014), which would account for the increased contribution of krill to snow petrel diet. The relatively restricted extent of the continental shelf at DML (<100 km) may make coastal polynya formation in this region particularly sensitive to ice-sheet advance.

The sustained presence of polynyas through MIS 3-2, as recorded in WMM7 and in other DML sequences (Fig. 6) (Berg et al., 2019) may also offer an explanation for the small amplitude of millennial-scale oscillations in sea-salt Na to the EPICA

ice core, and the weak relationship to Antarctic temperatures (Fischer et al., 2007). Although we show that polynya properties changed through time (Fig. 6), the open waters within the sea ice pack would have provided a continuous supply of sea-salt Na to the ice core site. Polynyas may also have affected the strength of the sea ice/climate feedbacks during MIS 2: introducing only 2-8% open waters into the LGM sea-ice pack (compared to 10-20% for winter today) reduces the Southern Ocean contribution to the LGM CO_2 draw-down from ~80% to 15-50% via enhanced ocean-atmosphere CO_2 transfer (Morales Maqueda and Rahmstorf, 2002). In contrast, increasing brine formation transfers dense water and carbon to the deep ocean (Bouttes et al., 2011), and could have been enhanced by polynya formation (Paillard and Parrenin, 2004 Brine formation over the continental shelves or at the ice-sheet margin has been proposed as , ~~either over the continental shelves or at the ice-sheet margin, would have been~~ conducive to formation of dense glacial AABW and the associated deep-ocean storage of CO_2 (Paillard and Parrenin, 2004; Adkins, 2013; Adkins et al., 2002). It is currently difficult to evaluate the relationship between the proposed variability in polynya positions and the millennial-scale oscillations in atmospheric CO_2 (Fig. 6), in part because it is unclear whether the variations in surface ocean productivity observed in the stomach-oil deposits are related to changes in the efficiency of the biological pump and CO_2 drawdown (e.g for Unit II with high chlorin inputs). Furthermore, the relative impact of polynyas compared to other Southern Ocean carbon cycle processes is unclear, given that a combination of brine formation related to sea ice growth, changes in deep ocean stratification, and iron fertilisation of subantarctic waters is invoked to account for the observed CO_2 drawdown (e.g. Bouttes et al., 2011; Marzocchi and Jansen, 2019; Sigman et al., 2021). The relative impact of the polynyas between winter and summer seasons during the last glacial stage is also uncertain, since the large changes in sea-ice extent (Fig. 1) will likely also have affected the air-sea gas exchange on seasonal timescales. Our age model uncertainties also limit confident correlation between WMM7 and the ice core CO_2 record, so that further testing is required to explore whether polynya development along the DML coastline impacted atmospheric CO_2.

5 Conclusions

Here, we present a multi-proxy analysis of stomach-oil deposits of snow petrels from Dronning Maud Land, Antarctica. We show that variation in trace metals and fatty acid distributions strongly suggest changes in snow petrel diet between 30.3-24.3 ~~28.8-22.6~~ ka. We show that, as today, a mixed diet of Antarctic krill and fish characterises much of the record. However, between 28.7-27.4 ~~26.8-25.7~~ cal. kyr BP signals of krill in the diet almost disappear. By linking dietary signals in the deposits to modern feeding habits and foraging ranges, we highlight the presence of open water ('polynyas') within more extensive summer sea-ice cover during MIS 2. The reduced contribution of Antarctic krill to the snow petrel diet between 28.7-27.4 ~~26.8-25.7~~ ka suggests restriction of polynyas to the continental shelf, limiting krill recruitment or access to waters where krill were present. Our results show that extensive, thick and multi-year sea ice was not always present close to the continent during MIS 2. These results add to a growing body of evidence which shows that seasonal changes in sea-ice extent and the presence of polynyas were likely important drivers of sea ice-climate feedbacks during glacial stages, whilst also highlighting the potential of stomach-oil deposits as a palaeoenvironmental archive of Southern Ocean conditions.~~challenge existing~~

~~hypotheses which emphasise multi-year sea ice as a key driver of positive sea ice-climate feedbacks during glacial stages, whilst also highlighting the potential of stomach-oil deposits as a palaeoenvironmental archive of Southern Ocean conditions.~~

660

Appendices

Table A1: comparison of radiocarbon calibrations. Calibration to calendar ages using MARINE13 (Reimer et al., 2013) and ΔR of 880 ± 100 yr (Björck et al. 1991; Sterken et al., 2012), as reported in the main text (Table 1), is compared to MARINE20 (Heaton et al., 2020) and updated ΔR of 670 ± 45 yr (Bjorck et al. 1991).

Sample depth, mm	Unit	AMS Lab ID	Median Age (^{14}C yr BP)	+/- (^{14}C yr BP)	Calibrated age (cal. yr BP) MARINE13, ΔR 880 ±100 yr	+/- (cal. yr BP, 2σ)	Calibrated age (cal. yr BP) MARINE20, ΔR 670 ±45 yr	+/- (cal. yr BP, 2σ)
surface	I	COL3022	21,550	110	22,400	894 / 383	22,140	318 / 377
0	I	COL4327	21,660	104	22,550	905 / 399	22,270	364 / 369
40	I	COL4326	23,170	114	24,160	637 / 272	23,910	271 / 329
79	I/II	COL4328	24,790	115	25,710	466 / 240	25,500	257 / 261
108	II/III	COL4329	25,980	133	26,780	786 / 385	26,740	369 / 351
135	III	COL4325	26,920	149	27,850	1085 / 497	27,680	415 / 333
160	III	COL4324	27,730	148	28,780	686 / 386	28,460	734 / 376

665

Figure ~~B~~A1: consistency of XRF scanning signals in deposit WMM7. The XRF data presented in Fig. 3 was recovered from a central slab of WMM7 (Fig. f), where we identified the longest sequence of horizontal laminae (Fig. 3). Here we show additional scans to investigate the internal consistency of the signals. Panels (a.-e.) correspond to lines (a.-e.) on panel f. Scans were undertaken to the left (b.) and right (d.) of the centre-line (c.), then two further cuts were used to investigate signals perpendicular to the cut surface (a. and e.). Away from the central line the signals are less strong and sometimes intermittent, but the laminae also dip sharply away from the centre (f.), suggesting more heterogenous accumulation, perhaps due to distance from the nest and/or nest morphology.
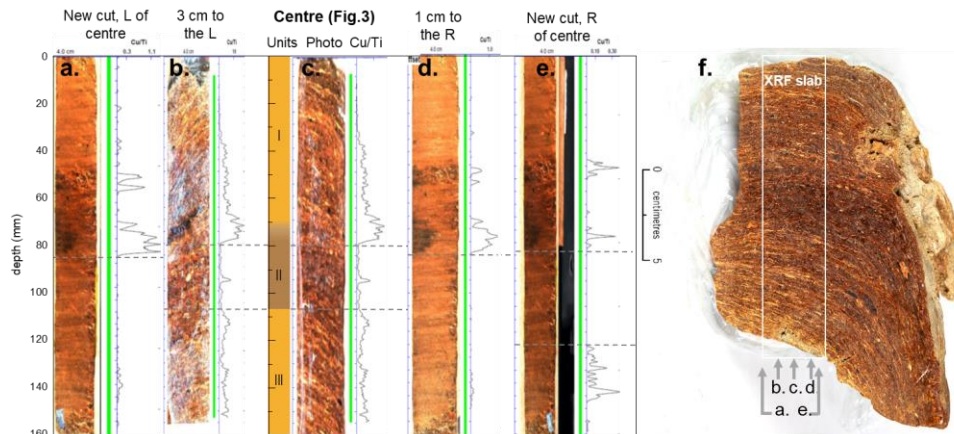
Figure ~~C~~B1: comparison of cluster analysis results for original XRF data, re-sampled XRF data (shown in Fig. 3) and organic indicator data (shown in Fig. 4). XRF data between 0-10 mm and 155-160 mm were removed before analysis.
680 **The left panel shows the original Cu/Ti data (grey line) with ~100 yr smoothing (orange line, as in Fig. 3), alongside re-sampled Cu/Ti data (orange squares) used for cluster analysis. The right panel shows the P410 pigment absorbance signal, which may account for the offset in the O1/O2 cluster boundary compared to 1/2 boundary in other analyses.**
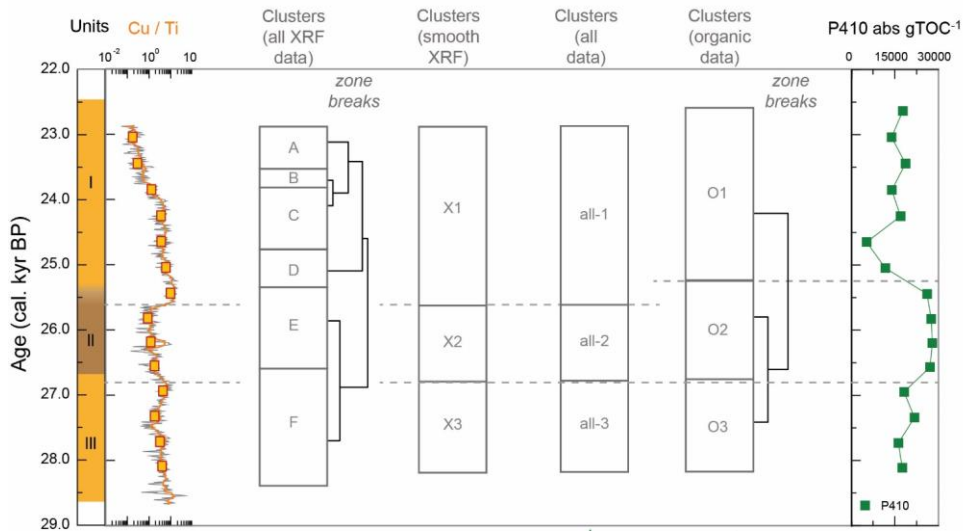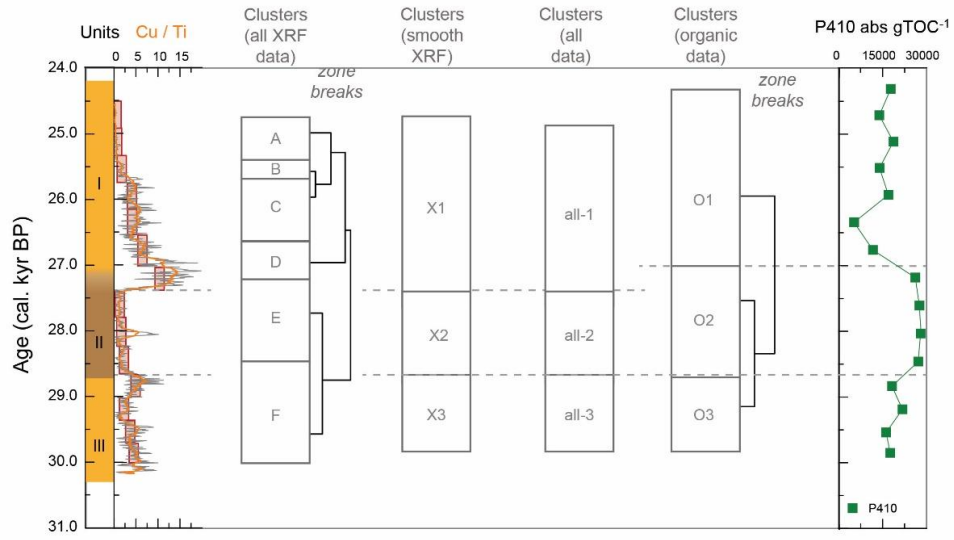
Figure ~~D~~C1: element contributions to stomach oil deposit WMM7, recorded by ITRAX XRF scanning (Croudace et al., 2006). Note that the amplitude of the signal decreases from left to right. Potential minerogenic (Ti, K, Al; brown), biogenic (Br, Zn, S, As; green) and mixed (Fe, Ca, Cu, Si; black) sources are noted. Cluster analysis was performed after removing data from 0-10 mm and 155-160 mm where several elements record values of zero.
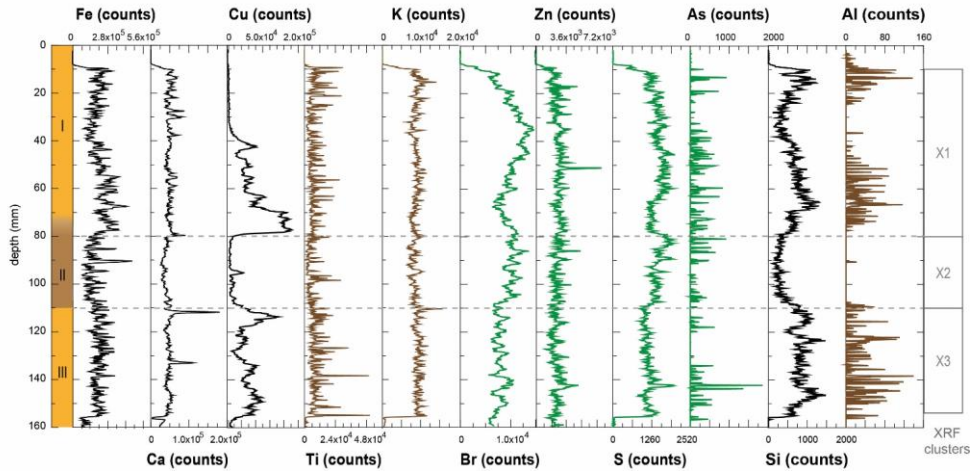
Figure ~~E~~D1: effect of normalisation for minerogenic inputs on the Fe and Cu signals in WMM7. Due to low or absent contributions of Al (Figure D1), data were normalised to Ti. Fe/Ti and Cu/Ti are shown here for comparison, as the original ratios and on a log scale. Fig. 3 presents all normalised XRF data on a log scale, excluding 0-10 mm and 155-160 mm, where very low counts of one or more element leads to anomalous values.
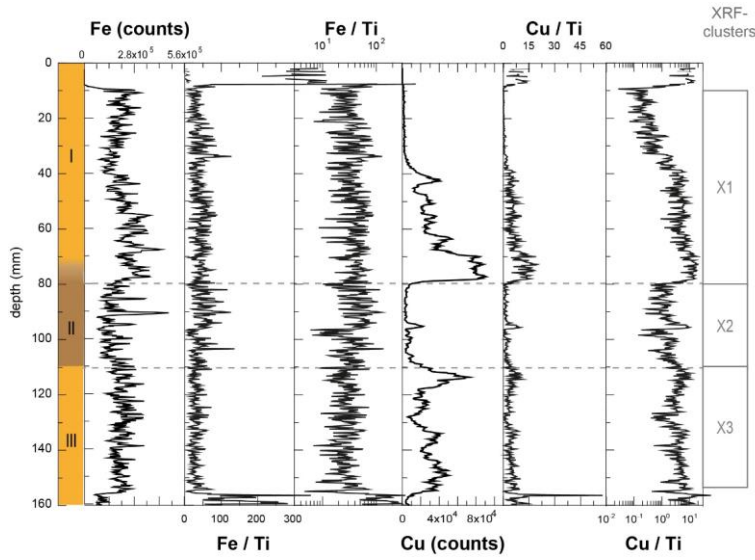
Figure FE1: additional indicators of organic matter composition of WMM7. The %N and %TOC were used to generate the C/N ratios presented in Fig. 4. The dominant pigments (P410, P435) are shown in comparison to the much lower contribution of P665, which has an exclusive chlorin origin but which is also 3 orders of magnitude lower in abundance than P410.
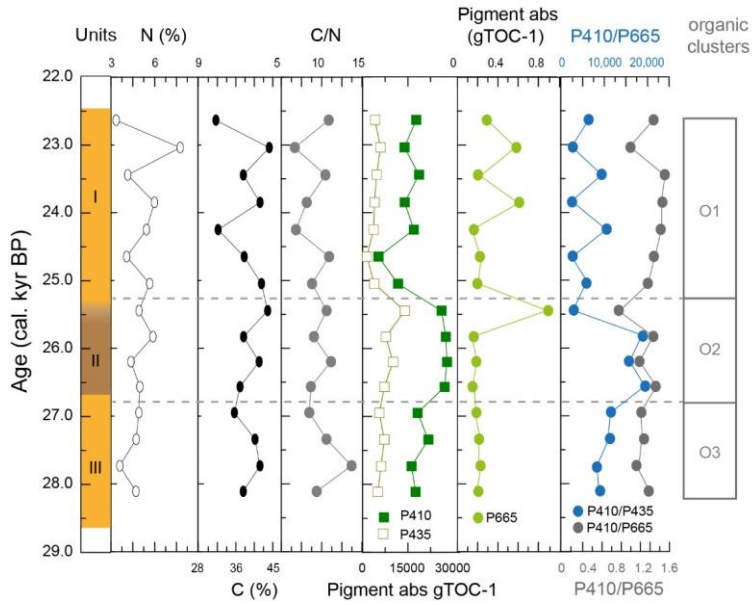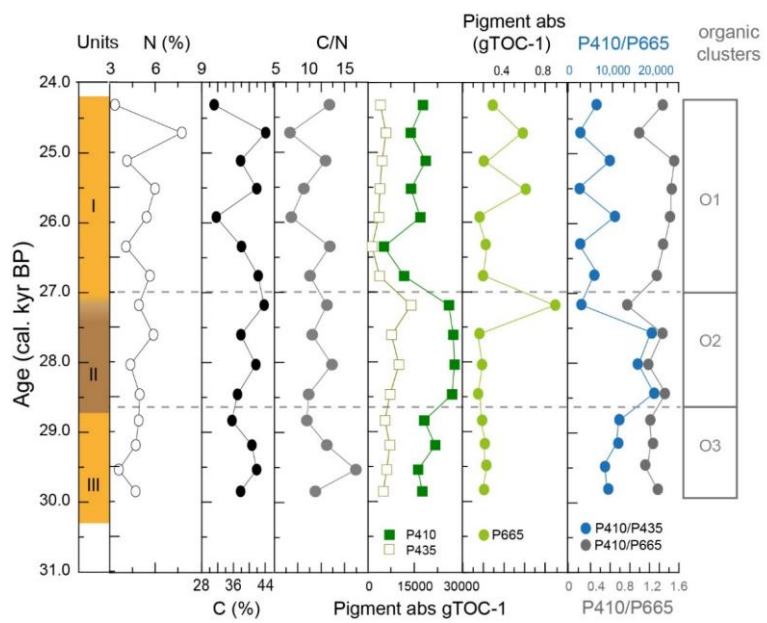
Data availability

710 All new proxy data presented here are available at https://doi.org/10.1594/PANGAEA.939211 (McClymont et al., 2021). ~~All data have been submitted to the PANGAEA repository. A DOI is pending.~~

Author contribution

ELM, MJB, DAH and GK designed the study. ELM, CSJ, MDW, TW, IC, SB and DG carried out the laboratory work and data analysis. ELM prepared the initial manuscript and interpretations in discussion with all authors. The final manuscript was
715 edited and reviewed by all authors.

Competing interests

The authors declare that they have no conflict of interest.

Acknowledgements

This project has received funding from the European Research Council (ERC) under the European Union's Horizon 2020
720 research and innovation programme (grant agreement n° 864637, "ANTSIE"), and from the Leverhulme Trust (Philip Leverhulme Prize and Research Leadership Award, ELM). This work was also supported by the Deutsche Forschungsgemeinschaft (DFG) in the framework of the priority program SPP 1158 "Antarctic Research with comparative investigations in Arctic ice areas" by the grant (BE4764/5-1; SB). Our thanks are given to U. Wand and W.-D. Hermichen for sampling, documentation and sample storage at the Alfred-Wegener-Institut Helmholtz-Zentrum für Polar- and
725 Meeresforschung research centre in Potsdam. We also thank Amanda Hayton and Kathryn Melvin for laboratory support at Durham University.

References

Ackley, S. F., Xie, H., and Tichenor, E. A.: Ocean heat flux under Antarctic sea ice in the Bellingshausen and Amundsen Seas:
730 two case studies, Annals of Glaciology, 56, 200-210, 2015.
Adkins, J. F., McIntyre, K., and Schrag, D. P.: The Salinity, Temperature, and delta 18O of the Glacial Deep Ocean, Science, 298, 1769-1773, 2002.
Adkins, J. F.: The role of deep ocean circulation in setting glacial climates, Paleoceanography, 28, 539-561, 10.1002/palo.20046, 2013.

735   Aiello, A., Fattorusso, E., Menna, M., Vitalone, R., Schröder, H. C., and Müller, W. E. G.: Mumijo traditional medicine: fossil deposits from antarctica (chemical composition and beneficial bioactivity), Evid Based Complement Alternat Med, 2011, 738131-738131, 10.1093/ecam/nen072, 2011.

Ainley, D. G., O'Connor, E. F., and Boekelheide, R. J.: The marine ecology of birds in the Ross Sea, Antarctica, in: American Ornithologist's Union Ornithological Monograph, 97, 1984.

740   Ainley, D. G., Ribic, C. A., and Fraser, W. R.: Does prey preference affect habitat choice in Antarctic seabirds?, Marine Ecology Progress Series, 90, 1992.

Ainley, D. G., Hobson, K. A., Crosta, X., Rau, G. H., Wassenaar, L. I., and Augustinus, P. C.: Holocene variation in the Antarctic coastal food web: linking δD and $\delta^{13}C$ in snow petrel diet and marine sediments, Marine Ecology Progress Series, 306, 31-40, 2006.

745   Allen, C. S., Pike, J., and Pudsey, C. J.: Last glacial-interglacial sea-ice cover in the SW Atlantic and its potential role in global deglaciation, Quaternary Science Reviews, 30, 2446-2458, 2011.

Arrigo, K. R., and van Dijken, G. L.: Phytoplankton dynamics within 37 Antarctic coastal polynya systems, Journal of Geophysical Research: Oceans, 108, 3271, 10.1029/2002JC001739, 2003.

Arrigo, K. R., van Dijken, G., and Long, M.: Coastal Southern Ocean: A strong anthropogenic CO2 sink, Geophysical Research
750   Letters, 35, L21602, 10.1029/2008GL035624, 2008.

Atkinson, A., Siegel, V., Pakhomov, E., and Rothery, P.: Long-term decline in krill stock and increase in salps within the Southern Ocean, Nature, 432, 100, 10.1038/nature02996.

Atkinson, A., Siegel, V., Pakhomov, E. A., Rothery, P., Loeb, V., Ross, R. M., Quetin, L. B., Schmidt, K., Fretwell, P., Murphy, E. J., Tarling, G. A., and Fleming, A. H.: Oceanic circumpolar habitats of Antarctic krill, Marine Ecology Progress Series,
755   362, 1-23, 2008.

Barbraud, C., Weimerskirch, H., Robertson, G. G., and Jouventin, P.: Size-related life history traits: insights from a study of snow petrels (Pagodroma nivea), Journal of Animal Ecology, 68, 1179-1192, https: //doi.org/10.1046/j.1365-2656.1999.00361.x, 1999.

Bennett, K.: Determination of the number of zones in a biostratigraphic sequence, New Phytologist, 132, 155-170, 1996.

760   Bentley, M. J., Ó Cofaigh, C., Anderson, J. B., Conway, H., Davies, B., Graham, A. G. C., Hillenbrand, C.-D., Hodgson, D. A., Jamieson, S. S. R., Larter, R. D., Mackintosh, A., Smith, J. A., Verleyen, E., Ackert, R. P., Bart, P. J., Berg, S., Brunstein, D., Canals, M., Colhoun, E. A., Crosta, X., Dickens, W. A., Domack, E., Dowdeswell, J. A., Dunbar, R., Ehrmann, W., Evans, J., Favier, V., Fink, D., Fogwill, C. J., Glasser, N. F., Gohl, K., Golledge, N. R., Goodwin, I., Gore, D. B., Greenwood, S. L., Hall, B. L., Hall, K., Hedding, D. W., Hein, A. S., Hocking, E. P., Jakobsson, M., Johnson, J. S., Jomelli, V., Jones, R. S.,
765   Klages, J. P., Kristoffersen, Y., Kuhn, G., Leventer, A., Licht, K., Lilly, K., Lindow, J., Livingstone, S. J., Massé, G., McGlone, M. S., McKay, R. M., Melles, M., Miura, H., Mulvaney, R., Nel, W., Nitsche, F. O., O'Brien, P. E., Post, A. L., Roberts, S. J., Saunders, K. M., Selkirk, P. M., Simms, A. R., Spiegel, C., Stolldorf, T. D., Sugden, D. E., van der Putten, N., van Ommen, T., Verfaillie, D., Vyverman, W., Wagner, B., White, D. A., Witus, A. E., and Zwartz, D.: A community-based geological

reconstruction of Antarctic Ice Sheet deglaciation since the Last Glacial Maximum, Quaternary Science Reviews, 100, 1-9, http: //dx.doi.org/10.1016/j.quascirev.2014.06.025, 2014.

Benz, V., Esper, O., Gersonde, R., Lamy, F., and Tiedemann, R.: Last Glacial Maximum sea surface temperature and sea-ice extent in the Pacific sector of the Southern Ocean, Quaternary Science Reviews, 146, 216-237, http: //dx.doi.org/10.1016/j.quascirev.2016.06.006, 2016.

Berg, S., Melles, M., Hermichen, W.-D., McClymont, E. L., Bentley, M. J., Hodgson, D. A., and Kuhn, G.: Evaluation of Mumiyo Deposits From East Antarctica as Archives for the Late Quaternary Environmental and Climatic History, Geochemistry, Geophysics, Geosystems, 20, 260-276, doi:10.1029/2018GC008054, 2019.

Bierman, W. H., and Voous, K. H.: Birds observed and collected during the whaling expedition of the 'Willem Barendz' in the Antarctic 1946–1947", Ardea 37, 1–123, 1950.

Björck, S., Hjort, C., Ingólfsson, O., and Skog, G.: Radiocarbon dates from the Antarctic Peninsula – problems and potential, in: Radiocarbon Dating: Recent Applications and Future Potential, edited by: Lowe, J. J., Quaternary Research Association, Cambridge, 55-65, 1991.

Bonn, W. J., Gingele, F. X., Grobe, H., Mackensen, A., and Fütterer, D. K.: Palaeoproductivity at the Antarctic continental margin: opal and barium records for the last 400 ka, Palaeogeography Palaeoclimatology Palaeoecology, 139, 195–211, 1998.

Bostock, H. C., Opdyke, B. N., Gagan, M. K., and Fifield, L. K.: Carbon isotope evidence for changes in Antarctic Intermediate Water circulation and ocean ventilation in the southwest Pacific during the last deglaciation, Paleoceanography, 19, 10.1029/2004PA001047, 2004

Bottino, N. R.: Lipid composition of two species of antarctic krill: Euphausia superba and E. crystallorophias, Comparative Biochemistry and Physiology Part B: Comparative Biochemistry, 50, 479-484, https://doi.org/10.1016/0305-0491(75)90261-8, 1975.

Bridges, C., Savel, A., Stöcker, W., J., M., and Linzen, B.: Structure and function of krill (*Euphausia superba*) haemocyanin—adaptation to life at low temperature, Life Chem Rep Suppl, 1, 353–356, 1983.

Cherel, Y., Fontaine, C., Richard, P., and Labatc, J.-P.: Isotopic niches and trophic levels of myctophid fishes and their predators in the Southern Ocean, Limnology and Oceanography, 55, 324-332, https: //doi.org/10.4319/lo.2010.55.1.0324, 2010.

Cherel, Y., Koubbi, P., Giraldo, C., Penot, F., Tavernier, E., Moteki, M., Ozouf-Costaz, C., Causse, R., Chartier, A., and Hosie, G.: Isotopic niches of fishes in coastal, neritic and oceanic waters off Adélie land, Antarctica, Polar Science, 5, 286-297, https: //doi.org/10.1016/j.polar.2010.12.004, 2011.

Collins, L. G., Pike, J., Allen, C. S., and Hodgson, D. A.: High-resolution reconstruction of southwest Atlantic sea-ice and its role in the carbon cycle during marine isotope stages 3 and 2, Paleoceanography, 27, PA3217, 10.1029/2011pa002264, 2012.

Collins, M., Knutti, R., Arblaster, J., Dufresne, J.-L., Fichefet, T., Friedlingstein, P., Gao, X., Gutowski, W. J., Johns, T., Krinner, G., Shongwe, M., Tebaldi, C., Weaver, A. J., and Wehner, M.: Long-term Climate Change: Projections, Commitments

and Irreversibility, in: Climate Change 2013: The Physical Science Basis. Contribution of Working Group I to the Fifth Assessment Report of the Intergovernmental Panel on Climate Change edited by: Stocker, T. F., Qin, D., Plattner, G.-K., Tignor, M., Allen, S. K., Boschung, J., Nauels, A., Xia, Y., Bex, V., and Midgley, P. M., Cambridge University Press, Cambridge, United Kingdom and New York, NY, USA., 2013.

Connan, M., Cherel, Y., and Mayzaud, P.: Lipids from stomach oil of procellariiform seabirds document the importance of myctophid fish in the Southern Ocean, Limnology and Oceanography, 52, 2445-2455, 2007.

Cripps, G. C., Watkins, J. L., Hill, H. J., and Atkinson, A.: Fatty acid content of Antarctic krill *Euphausia superba* at South Georgia related to regional populations and variations in diet, Marine Ecology Progress Series, 181, 177-188, 1999.

Crosta, X., and Shemesh, A.: Reconciling down core anticorrelation of diatom carbon and nitrogen isotopic ratios from the Southern Ocean, 17, 10-11-10-18, 10.1029/2000pa000565, 2002.

Croudace, I. W., Rindby, A., and Rothwell, R. G.: ITRAX: Description and evaluation of a new sediment core scanner, in: New techniques in sediment core analysis, edited by: Rothwell, R. G., Geological Society Special Publication, 267, 51-63, 2006.

Delille, B., Vancoppenolle, M., Geilfus, N.-X., Tilbrook, B., Lannuzel, D., Schoemann, V., Becquevort, S., Carnat, G., Delille, D., Lancelot, C., Chou, L., Dieckmann, G. S., and Tison, J.-L.: Southern Ocean CO_2 sink: The contribution of the sea ice, Journal of Geophysical Research: Oceans, 119, 6340-6355, 10.1002/2014JC009941, 2014.

Delmont, T. O., Hammar, K. M., Ducklow, H. W., Yager, P. L., and Post, A. F.: *Phaeocystis antarctica* blooms strongly influence bacterial community structures in the Amundsen Sea polynya, Frontiers in Microbiology, 5, 10.3389/fmicb.2014.00646, 2014.

Delord, K., Pinet, P., Pinaud, D., Barbraud, C., De Grissac, S., Lewden, A., Cherel, Y., and Weimerskirch, H.: Species-specific foraging strategies and segregation mechanisms of sympatric Antarctic fulmarine petrels throughout the annual cycle, Ibis, 158, 569-586, 10.1111/ibi.12365, 2016.

Dunbar, R. B., and Leventer, A.: Seasonal variation in carbon isotopic composition of antarctic sea ice and open-water plankton communities, Antarctic Journal of the United States, 27, 79-81, 1992.

Falla, R. A.: Birds, 1-288, 1937.

Färber Lorda, J., and Ceccaldi, H. J.: Relationship of morphometrics, total carotenoids, and total lipids with activity and sexual and spatial features in Euphausia superba, Scientific Reports, 10, 13177, 10.1038/s41598-020-69780-8, 2020.

Ferrari, R., Jansen, M. F., Adkins, J. F., Burke, A., Stewart, A. L., and Thompson, A. F.: Antarctic sea ice control on ocean circulation in present and glacial climates, Proceedings of the National Academy of Sciences, 111, 8753-8758, 10.1073/pnas.1323922111, 2014.

Fijn, R. C., van Franeker, J. A., and Trathan, P. N.: Dietary variation in chick-feeding and self-provisioning Cape Petrel Daption capense and Snow Petrel *Pagodroma nivea* at Signy Island, South Orkney Islands, Antarctica, Marine Ornithology, 40, 81-87, 2012.

Fischer, H., Fundel, F., Ruth, U., Twarloh, B., Wegner, A., Udisti, R., Becagli, S., Castellano, E., Morganti, A., Severi, M., Wolff, E., Littot, G., Rothlisberger, R., Mulvaney, R., Hutterli, M. A., Kaufmann, P., Federer, U., Lambert, F., Bigler, M., Hansson, M., Jonsell, U., de Angelis, M., Boutron, C., Siggaard-Andersen, M.-L., Steffensen, J. P., Barbante, C., Gaspari, V., Gabrielli, P., and Wagenbach, D.: Reconstruction of millennial changes in dust emission, transport and regional sea ice coverage using the deep EPICA ice cores from the Atlantic and Indian Ocean sector of Antarctica, Earth and Planetary Science Letters, 260, 340-354, 2007.

Francois, R., Altabet, M. A., Goericke, R., McCorkle, D. C., Brunet, C., and Poisson, A.: Changes in the $\delta^{13}C$ of surface water particulate organic matter across the subtropical convergence in the SW Indian Ocean, Global Biogeochemical Cycles, 7, 627-644, https://doi.org/10.1029/93GB01277, 1993.

Friedrich, C., and Hagen, W.: Lipid contents of five species of notothenioid fish from high-Antarctic waters and ecological implications, Polar Biology, 14, 359-369, 10.1007/BF00240256, 1994.

Frölicher, T. L., Joos, F., and Raible, C. C.: Sensitivity of atmospheric CO_2 and climate to explosive volcanic eruptions, Biogeosciences, 8, 2317-2339, doi: 2310.5194/bg-2318-2317-2011, 2011.

Gersonde, R., Abelmann, A., Brathauer, U., Becquey, S., Bianchi, C., Cortese, G., Grobe, H., Kuhn, G., Niebler, H.-S., Segl, M., Sieger, R., Zielinski, U., and Fütterer, D. K.: Last glacial sea surface temperatures and sea-ice extent in the Southern Ocean (Atlantic-Indian Sector): A multiproxy approach, Paleoceanography, 18, 1061, 2003.

Gersonde, R., Crosta, X., Abelmann, A., and Armand, L.: Sea-surface temperature and sea ice distribution of the Southern Ocean at the EPILOG Last Glacial Maximum--a circum-Antarctic view based on siliceous microfossil records, Quaternary Science Reviews, 24, 869-896, 2005.

Goto-Azuma, K., Hirabayashi, M., Motoyama, H., Miyake, T., Kuramoto, T., Uemura, R., Igarashi, M., Iizuka, Y., Sakurai, T., Horikawa, S., Suzuki, K., Suzuki, T., Fujita, K., Kondo, Y., Hattori, S., and Fujii, Y.: Reduced marine phytoplankton sulphur emissions in the Southern Ocean during the past seven glacials, Nature Communications, 10, 3247, 10.1038/s41467-019-11128-6, 2019.

Grobe, H., and Mackensen, A.: Late Quaternary climatic cycles as recorded in sediments from the Antarctic continental margin, in: The Antarctic Paleoenvironment: a Perspective on Global Change, edited by: Kennett, J. P., and Warnke, D. A., Antarctic Research Series vol. 56, American Geophysical Union, Washington DC, 349-376, 1993.

Hammer, Ø., Harper, D. A. T., and Ryan, P. D.: PAST: Paleontological Statistics Software Package for Education and Data Analysis, Palaeontologia Electronica, 4, 9pp., 2001.

Harris, P. G., and Maxwell, J. R.: A novel method for the rapid determination of chlorin concentrations at high stratigraphic resolution in marine sediments, Organic Geochemistry, Submitted, 1995.

Heaton, T. J., Köhler, P., Butzin, M., Bard, E., Reimer, R. W., Austin, W. E. N., Bronk Ramsey, C., Grootes, P. M., Hughen, K. A., Kromer, B., Reimer, P. J., Adkins, J., Burke, A., Cook, M. S., Olsen, J., and Skinner, L. C.: Marine20—The Marine Radiocarbon Age Calibration Curve (0–55,000 cal BP), Radiocarbon, 62, 779-820, 10.1017/RDC.2020.68, 2020.

870   Heaton, T. J., Bard, E., Ramsey, C. B., Butzin, M., Köhler, P., and Reimer, P. J.: Comment on cp-2021-134, Climate of the Past Discussion, https://doi.org/10.5194/cp-2021-134-CC1, 2021.

Henley, S. F., Annett, A. L., Ganeshram, R. S., Carson, D. S., Weston, K., Crosta, X., Tait, A., Dougans, J., Fallick, A. E., and Clarke, A.: Factors influencing the stable carbon isotopic composition of suspended and sinking organic matter in the coastal

875   Antarctic sea ice environment, Biogeosciences, 9, 1137-1157, 10.5194/bg-9-1137-2012, 2012.

Hillenbrand, C.-D., and Cortese, G.: Polar stratification: A critical view from the Southern Ocean, Palaeogeography, Palaeoclimatology, Palaeoecology, 242, 240-252, http: //dx.doi.org/10.1016/j.palaeo.2006.06.001, 2006.

Hillenbrand, C.-D., Bentley, M. J., Stolldorf, T. D., Hein, A. S., Kuhn, G., Graham, A. G. C., Fogwill, C. J., Kristoffersen, Y., Smith, J. A., Anderson, J. B., Larter, R. D., Melles, M., Hodgson, D. A., Mulvaney, R., and Sugden, D. E.: Reconstruction of

880   changes in the Weddell Sea sector of the Antarctic Ice Sheet since the Last Glacial Maximum, Quaternary Science Reviews, 100, 111-136, http: //dx.doi.org/10.1016/j.quascirev.2013.07.020, 2014.

Hiller, A., Wand, U., Kampft, H., and Stackebrandt, W.: Occupation of the Antarctic Continent by Petrels During the Past 35 000 Years: Inferences from a [14]C Study of Stomach Oil Deposits, Polar Biology, 9, 69-77, 1988.

Hiller, A., Hermichen, W.-D., and Wand, U.: Radiocarbon-dated subfossil stomach oil deposits from petrel nesting sites: novel

885   paleoenvironmental records from continental Antarctica, Radiocarbon, 37, 171-180, 1995.

Horgan, I. E., and Barrett, J. A.: The Use of Lipid Profiles in Comparing the Diet of Seabirds, in: Antarctic Nutrient Cycles and Food Webs, edited by: Siegfried, W. R., Condy, P. R., and Laws, R. M., Springer Berlin Heidelberg, Berlin, Heidelberg, 493-497, 1985.

Huang, T., Sun, L., Wang, Y., Liu, X., and Zhu, R.: Penguin population dynamics for the past 8500 years at Gardner Island,

890   Vestfold Hills, Antarctic Science, 21, 571-578, 10.1017/S0954102009990332, 2009.

Imber, M. J.: The Origin of Petrel Stomach Oils: A Review, The Condor, 78, 366-369, 10.2307/1367697, 1976.

Jaeger, A., and Cherel, Y.: Isotopic Investigation of Contemporary and Historic Changes in Penguin Trophic Niches and Carrying Capacity of the Southern Indian Ocean, PLOS ONE, 6, e16484, 10.1371/journal.pone.0016484, 2011.

Jeffrey, S. W., Mantoura, R. F. C., and BjØrnland, T.: Data for the identification of 47 key phytoplankton pigments, in:

895   Phytoplankton pigments in oceanography: guidelines to modern methods, edited by: Jeffrey, S. W., Mantoura, R. F. C., and Wright, S. W., 149-559, 1997.

Johansson, P., and Thor, G.: Observations on the birds of the Vestfjella and Heimefrontfjella, Dronning Maud Land, Antarctica, 1991/92 and 2001/02, Marine Ornithology, 32, 43-46, 2004.

Jónasdóttir, S. H.: Fatty Acid Profiles and Production in Marine Phytoplankton, 17, 151, 2019.

900   Karnovsky, N., Ainley, D. G., and Lee, P.: Chapter 12 The Impact and Importance of Production in Polynyas to Top-Trophic Predators: Three Case Histories, in: Elsevier Oceanography Series, edited by: Smith, W. O., and Barber, D. G., Elsevier, 391-410, 2007.

Ju, S.-J., and Harvey, H. R.: Lipids as markers of nutritional condition and diet in the Antarctic krill Euphausia superba and Euphausia crystallorophias during austral winter, Deep Sea Research Part II: Topical Studies in Oceanography, 51, 2199-2214, https://doi.org/10.1016/j.dsr2.2004.08.004, 2004.

Juggins, S. (2020). rioja: Analysis of Quaternary Science Data. R package version 0.9-26: https://cran.r-project.org/package=rioja.

Kennedy, H., Thomas, D., Kattner, G., Haas, C., and Dieckmann, G.: Particulate organic matter in Antarctic summer sea ice: Concentration and stable isotopic composition, Marine Ecology Progress Series, 238, 1-13, 2002.

Lee, H., Feakins, S. J., Lu, Z., Schimmelmann, A., Sessions, A. L., Tierney, J. E., and Williams, T. J.: Comparison of three methods for the methylation of aliphatic and aromatic compounds, Rapid Commun Mass Spectrom, 31, 1633-1640, 10.1002/rcm.7947, 2017.

Lee, R. F., Nevenzel, J. C., and Paffenhöfer, G. A.: Importance of wax esters and other lipids in the marine food chain: Phytoplankton and copepods, Marine Biology, 9, 99-108, 10.1007/BF00348249, 1971.

Leri, A. C., Hakala, J. A., Marcus, M. A., Lanzirotti, A., Reddy, C. M., and Myneni, S. C. B.: Natural organobromine in marine sediments: New evidence of biogeochemical Br cycling, Global Biogeochemical Cycles, 24, https://doi.org/10.1029/2010GB003794, 2010.

Lewis, R. W.: Studies of the glyceryl ethers of the stomach oil of Leach's petrel *Oceanodroma leucorhoa* (Viellot), Comp. Biochem. Physiol., 19, 363-377, 1966.

Liu, X., Nie, Y., Sun, L., and Emslie, S. D.: Eco-environmental implications of elemental and carbon isotope distributions in ornithogenic sediments from the Ross Sea region, Antarctica, Geochimica et Cosmochimica Acta, 117, 99-114, https://doi.org/10.1016/j.gca.2013.04.013, 2013.

Lucchi, R. G., Rebesco, M., Camerlenghi, A., Busetti, M., Tomadin, L., Villa, G., Persico, D., Morigi, C., Bonci, M. C., and Giorgetti, G.: Mid-late Pleistocene glacimarine sedimentary processes of a high-latitude, deep-sea sediment drift (Antarctic Peninsula Pacific margin), Marine Geology, 189, 343-370, http: //dx.doi.org/10.1016/S0025-3227(02)00470-X, 2002.

Mackensen, A., Grobe, H., Hubberton, H.-W., Spiess, V., and Futterer, D. K.: Stable isotope stratigraphy from the Antarctic continental margin during the last one million years, Marine Geology, 87, 315-321, 1989.

Mackintosh, A. N., Verleyen, E., O'Brien, P. E., White, D. A., Jones, R. S., McKay, R., Dunbar, R., Gore, D. B., Fink, D., Post, A. L., Miura, H., Leventer, A., Goodwin, I., Hodgson, D. A., Lilly, K., Crosta, X., Golledge, N. R., Wagner, B., Berg, S., van Ommen, T., Zwartz, D., Roberts, S. J., Vyverman, W., and Masse, G.: Retreat history of the East Antarctic Ice Sheet since the Last Glacial Maximum, Quaternary Science Reviews, 100, 10-30, http: //dx.doi.org/10.1016/j.quascirev.2013.07.024, 2014.

Mayzaud, P., Chevallier, J., Tavernier, E., Moteki, M., and Koubbi, P.: Lipid composition of the Antarctic fish *Pleuragramma antarcticum*. Influence of age class, Polar Science, 5, 264-271, https: //doi.org/10.1016/j.polar.2010.12.003, 2011.

McClymont, E. L., Martinez-Garcia, A., and Rosell-Mele, A.: Benefits of freeze-drying sediments for the analysis of total chlorins and alkenone concentrations in marine sediments, Organic Geochemistry, 38, 1002-1007, doi:1010.1016/j.orggeochem.2007.1001.2006, 2007.

McClymont, E. L., et al. (2021). Age model, XRF data, fatty acid distributions and stable isotope analysis for stomach oil deposit WMM7, Dronning Maud Land. . PANGAEA, https://doi.org/10.1594/PANGAEA.939211.

Menviel, L., Mouchet, A., Meissner, K. J., Joos, F., and England, M. H.: Impact of oceanic circulation changes on atmospheric $\delta^{13}CO_2$, Global Biogeochemical Cycles, 29, 1944-1961, https://doi.org/10.1002/2015GB005207, 2015.

Mills, W. F., Xavier, J. C., Bearhop, S., Cherel, Y., Votier, S. C., Waluda, C. M., and Phillips, R. A.: Long-term trends in albatross diets in relation to prey availability and breeding success, Marine Biology, 167, 29, 10.1007/s00227-019-3630-1, 2020.

Mills, W. F., Morley, T. I., Votier, S. C., and Phillips, R. A.: Long-term inter- and intraspecific dietary variation in sibling seabird species, Marine Biology, 168, 31, 10.1007/s00227-021-03839-6, 2021.

Mohrmann, M., Heuzé, C., and Swart, S.: Southern Ocean polynyas in CMIP6 models, The Cryosphere Discuss., 2021, 1-43, 10.5194/tc-2021-23, 2021.

Morales Maqueda, M. A., and Rahmstorf, S.: Did Antarctic sea-ice expansion cause glacial CO2 decline?, Geophysical Research Letters, 29, 11-11-11-13, 10.1029/2001GL013240, 2002.

Morales Maqueda, M. A., Willmott, A. J., and Biggs, N. R. T.: Polynya Dynamics: a Review of Observations and Modeling, Reviews of Geophysics, 42, RG1004, 10.1029/2002RG000116, 2004.

Mychra, A., and Tatur, A.: Ecological role of the current and abandoned penguin rookeries in the land environment of the maritime Antarctic, Polish Polar Research, 12, 3–24, 1991.

Nicol, S.: A comparison of Antarctic petrel (*Thalassoica antarctica*) diets with net samples of Antarctic krill (*Euphausia superba*) taken from the Prydz Bay region, Polar Biology, 13, 399-403, 1993.

Nicol, S.: Krill, Currents, and Sea Ice: *Euphausia superba* and Its Changing Environment, BioScience, 56, 111-120, 10.1641/0006-3568(2006)056[0111: KCASIE]2.0.CO; 2, 2006.

Olivier, F., van Franeker, J. A., Creuwels, J. C. S., and Woehler, E. J.: Variations of snow petrel breeding success in relation to sea-ice extent: detecting local response to large-scale processes?, Polar Biology, 28, 687-699, 2005.

Olivier, F., and Wotherspoon, S. J.: Modelling habitat selection using presence-only data: Case study of a colonial hollow nesting bird, the snow petrel, Ecological Modelling, 195, 187-204, https: //doi.org/10.1016/j.ecolmodel.2005.10.036, 2006.

Paillard, D., and Parrenin, F.: The Antarctic ice sheet and the triggering of deglaciations, Earth and Planetary Science Letters, 227, 263-271, 2004.

Palmer Locarnini, S. J., and Presley, B. J.: Trace element concentrations in Antarctic krill, *Euphausia superba*, Polar Biology, 15, 283-288, 10.1007/BF00239849, 1995.

Parkinson, C. L.: A 40-y record reveals gradual Antarctic sea ice increases followed by decreases at rates far exceeding the rates seen in the Arctic, Proceedings of the National Academy of Sciences, 116, 14414-14423, 10.1073/pnas.1906556116, 2019.

Phillips, R. A., Bearhop, S., McGill, R. A., and Dawson, D. A.: Stable isotopes reveal individual variation in migration strategies and habitat preferences in a suite of seabirds during the nonbreeding period, Oecologia, 160, 795-806, 10.1007/s00442-009-1342-9, 2009.

Phillips, R. A., McGill, R. A. R., Dawson, D. A., and Bearhop, S.: Sexual segregation in distribution, diet and trophic level of seabirds: insights from stable isotope analysis, Marine Biology, 158, 2199-2208, 2011.

Polito, M. J., Trivelpiece, W. Z., Karnovsky, N. J., Ng, E., Patterson, W. P., and Emslie, S. D.: Integrating Stomach Content and Stable Isotope Analyses to Quantify the Diets of Pygoscelid Penguins, PLOS ONE, 6, e26642, 10.1371/journal.pone.0026642, 2011.

Post, D. M.: Using Stable Isotopes to Estimate Trophic Position: Models, Methods, and Assumptions, Ecology, 83, 703-718, 10.2307/3071875, 2002.

Quillfeldt, P., and Masello, J. F.: Compound-specific stable isotope analyses in Falkland Islands seabirds reveal seasonal changes in trophic positions, BMC Ecology, 20, 21, 10.1186/s12898-020-00288-5, 2020.

Raclot, T., Groscolas, R., and Cherel, Y.: Fatty acid evidence for the importance of myctophid fishes in the diet of king penguins, *Aptenodytes patagonicus*, Marine Biology, 132, 523-533, 10.1007/s002270050418, 1998.

Rae, J. W. B., Burke, A., Robinson, L. F., Adkins, J. F., Chen, T., Cole, C., Greenop, R., Li, T., Littley, E. F. M., Nita, D. C., Stewart, J. A., and Taylor, B. J.: CO_2 storage and release in the deep Southern Ocean on millennial to centennial timescales, Nature, 562, 569-573, 10.1038/s41586-018-0614-0, 2018.

Rainbow, P. S.: Copper, cadmium and zinc concentrations in oceanic amphipod and euphausiid crustaceans, as a source of heavy metals to pelagic seabirds, Marine Biology, 103, 513-518, 10.1007/BF00399583, 1989.

Rau, G. H., Ainley, D. G., Bengtson, J. L., Torres, J. J., and Hopkins, T. L.:$^{15}N/^{14}N$ and $^{13}C/^{12}C$ in Weddell Sea birds, seals, and fish: implications for diet and trophic structure, Marine Ecology Progress Series, 84, 1-8, 1992.

Reimer, P. J., Bard, E., Bayliss, A., Beck, J. W., Blackwell, P. G., Ramsey, C. B., Buck, C. E., Cheng, H., Edwards, R. L., Friedrich, M., Grootes, P. M., Guilderson, T. P., Haflidason, H., Hajdas, I., Hatté, C., Heaton, T. J., Hoffmann, D. L., Hogg, A. G., Hughen, K. A., Kaiser, K. F., Kromer, B., Manning, S. W., Niu, M., Reimer, R. W., Richards, D. A., Scott, E. M., Southon, J. R., Staff, R. A., Turney, C. S. M., and van der Plicht, J.: IntCal13 and Marine13 Radiocarbon Age Calibration Curves 0–50,000 Years cal BP, Radiocarbon, 55, 1869-1887, 10.2458/azu_js_rc.55.16947, 2013.

Rethemeyer, J., Gierga, M., Heinze, S., Stolz, A., Wotte, A., Wischhöfer, P., Berg, S., Melchert, J., Dewald, A.: Current sample preparation and analytical capabilities of the radiocarbon laboratory at CologneAMS. Radiocarbon, DOI: 10.1017/RDC.2019.16, 2019.

Ridoux, V., and Offredo, C.: The diets of five summer breeding seabirds in Adélie Land, Antarctica, Polar Biology, 9, 137-145, 10.1007/bf00297168, 1989.

Roche, D. M., Crosta, X., and Renssen, H.: Evaluating Southern Ocean sea-ice for the Last Glacial Maximum and pre-industrial climates: PMIP-2 models and data evidence, Quaternary Science Reviews, 56, 99-106, http: //dx.doi.org/10.1016/j.quascirev.2012.09.020, 2012.

Saunders, R. A., Hill, S. L., Tarling, G. A., and Murphy, E. J.: Myctophid Fish (Family Myctophidae) Are Central Consumers in the Food Web of the Scotia Sea (Southern Ocean), Frontiers in Marine Science, 6, 10.3389/fmars.2019.00530, 2019.

Seyboth, E., Botta, S., Mendes, C. R. B., Negrete, J., Dalla Rosa, L., and Secchi, E. R.: Isotopic evidence of the effect of warming on the northern Antarctic Peninsula ecosystem, Deep Sea Research Part II: Topical Studies in Oceanography, 149, 218-228, 2018.

Sherrell, R., Lagerström, M., Forsch, K., Stammerjohn, S., and Yager, P.: Dynamics of dissolved iron and other bioactive trace metals (Mn, Ni, Cu, Zn) in the Amundsen Sea Polynya, Antarctica, Elementa: Science of the Anthropocene, 3, 000071. doi:000010.012952/journal.elementa.000071, 2015.

Smith, J. A., Hillenbrand, C.-D., Pudsey, C. J., Allen, C. S., and Graham, A. G. C.: The presence of polynyas in the Weddell Sea during the Last Glacial Period with implications for the reconstruction of sea-ice limits and ice sheet history, Earth and Planetary Science Letters, 296, 287-298, http: //dx.doi.org/10.1016/j.epsl.2010.05.008, 2010.

Sprenk, D., Weber, M. E., Kuhn, G., Wennrich, V., Hartmann, T., and Seelos, K.: Seasonal changes in glacial polynya activity inferred from Weddell Sea varves, Clim. Past, 10, 1239-1251, 10.5194/cp-10-1239-2014, 2014.

Steele, W. K.: Stable isotope ratios of Antarctic petrel (*Thallassoica antarctica*) and snow petrel (*Pagodroma nivea*) bone collagen, Polar Biology, 28, 672-679, 2005.

Stephens, B. B., and Keeling, R. F.: The influence of Antarctic sea ice on glacial-interglacial CO_2 variations, Nature, 404, 171-174, 2000.

~~Sterken, M., Roberts, S. J., Hodgson, D. A., Vyverman, W., Balbo, A. L., Sabbe, K., Moreton, S. G., and Verleyen, E.: Holocene glacial and climate history of Prince Gustav Channel, northeastern Antarctic Peninsula, Quaternary Science Reviews, 31, 93-111, https://doi.org/10.1016/j.quascirev.2011.10.017, 2012.~~

Thatje, S., Hillenbrand, C.-D., Mackensen, A., and Larter, R.: Life Hung by a Thread: Endurance of Antarctic Fauna in Glacial Periods, Ecology, 89, 682-692, 2008.

Thor, G., and Low, M.: The persistence of the snow petrel (*Pagodroma nivea*) in Dronning Maud Land (Antarctica) for over 37,000 years, Polar Biology, 34, 609-613, 10.1007/s00300-010-0912-y, 2011.

Tierney, J. E., Zhu, J., King, J., Malevich, S. B., Hakim, G. J., and Poulsen, C. J.: Glacial cooling and climate sensitivity revisited, Nature, 584, 569-573, 10.1038/s41586-020-2617-x, 2020.

Trull, T. W., and Armand, L.: Insights into Southern Ocean carbon export from the $\delta^{13}C$ of particles and dissolved inorganic carbon during the SOIREE iron release experiment, Deep Sea Research Part II: Topical Studies in Oceanography, 48, 2655-2680, https: //doi.org/10.1016/S0967-0645(01)00013-3, 2001.

1035 Turner, J., Guarino, M. V., Arnatt, J., Jena, B., Marshall, G. J., Phillips, T., Bajish, C. C., Clem, K., Wang, Z., Andersson, T., Murphy, E. J., and Cavanagh, R.: Recent Decrease of Summer Sea Ice in the Weddell Sea, Antarctica, Geophysical Research Letters, 47, e2020GL087127, https: //doi.org/10.1029/2020GL087127, 2020.

Vallet, C., Beans, C., Koubbi, P., Courcot, L., Hecq, J.-H., and Goffart, A.: Food preferences of larvae of Antarctic silverfish Pleuragramma antarcticum Boulenger, 1902 from Terre Adélie coastal waters during summer 2004, Polar Science, 5, 239-
1040 251, https: //doi.org/10.1016/j.polar.2010.12.005, 2011.

Wand, U., and Hermichen, W.-D.: Late Quaternary Ice Level Changes in Central Dronning Maud Land, East Antarctica, as Inferred from ^{14}C ages of Mumiyo Deposits in Snow Petrel Colonies, Geol Jahrbuch, B97, 237-254, 2005.

Wang, S. W., Iverson, S. J., Springer, A. M., and Hatch, S. A.: Fatty acid signatures of stomach oil and adipose tissue of northern fulmars (*Fulmarus glacialis*) in Alaska: implications for diet analysis of Procellariiorm birds, J. Comp. Physiol. B,
1045 177, 893-903, 2007.

Warham, J., Watts, R., and Dainty, R. J.: The composition, energy content and function of the stomach oils of petrels (order, Procellariiformes), J. exp. mar. Biol. Ecol., 23, 1-13, 1976.

Warham, J.: The incidence, functions and ecological significance of petrel stomach oils, Proceedings of the New Zealand Ecological Society, 24, 84–93, 1977.
1050 Watanabe, Y. Y., Ito, K., Kokubun, N., and Takahashi, A.: Foraging behavior links sea ice to breeding success in Antarctic penguins, Science Advances, 6, eaba4828, 10.1126/sciadv.aba4828, 2020.

Watanuki, Y., and Thiebot, J.-B.: Factors affecting the importance of myctophids in the diet of the world's seabirds, Marine Biology, 165, 79, 10.1007/s00227-018-3334-y, 2018.

Watts, R., and Warham, J.: Structure of some intact lipids of petrel stomach oils, Lipids, 11, 423-429, 10.1007/bf02532831,
1055 1976.

Weber, M. E., Bonani, G., and Fütterer, K. D.: Sedimentation processes within channel-ridge systems, southeastern Weddell Sea, Antarctica, Paleoceanography, 9, 1027-1048, 1994.

Xiao, W., Esper, O., and Gersonde, R.: Last Glacial - Holocene climate variability in the Atlantic sector of the Southern Ocean,
1060 Quaternary Science Reviews, 135, 115-137, https: //doi.org/10.1016/j.quascirev.2016.01.023, 2016.